1319450

CHAN, KWOK WAH

AN AUTOMATED THERMISTOR CALIBRATION SYSTEM

The University of Arizona M.S. 1982

University
Microfilms
International 300 N. Zeeb Road, Ann Arbor, MI 48106

AN AUTOMATED THERMISTOR CALIBRATION SYSTEM

by

Chan Kwok Wah

A Thesis Submitted to the Faculty of the

DEPARTMENT OF ELECTRICAL ENGINEERING

In Partial Fulfillment of the Requirements
For the Degree of

MASTER OF SCIENCE

In the Graduate College

THE UNIVERSITY OF ARIZONA

1 9 8 2

STATEMENT BY AUTHOR

This thisis has been submitted in partial fulfillment of requirements for an advanced degree at The University of Arizona and is deposited in the University Library to made available to borrowers under rules of the Library.

Brief quotations from this thesis are allowable without special permission, provided that accurate acknowledgment of source is made. Requests for permission for extended quotations from or reproduction of this manuscript in whole or in part may be granted by the head of the major department or the Dean of the Graduate College when in his judgment the proposed use of the material is in the interests of scholarship. In all other instances, however, permission must be obtained from the author.

SIGNED: Khan Farooq Zeb

APPROVAL BY THESIS DIRECTOR

This thesis has been approved on the date shown below:

T. C. Cetas

T. C. CETAS
Adjunct Associate Professor of
Electrical Engineering
Associate Professor of Radiology

7/13/82
Date

ACKNOWLEDGEMENT

The author would like to express his sincere appreciation to his advisor, Dr. Thomas C. Cetas, for his gudiance and support throughout the various stages of this project. Thanks to Ms. Anne Fletcher for her assistance in preparing the drawings for this manuscript and Cyn Utter for her kindness in providing the word processor for doing this manuscript. Finally, the author wishes to express a very special gratitude to his very best friend Lilja, for her encouragement throughout this entire project.

TABLE OF CONTENTS

TABLE OF CONTENTS--continued

LIST OF TABLES

LIST OF ILLUSTRATIONS

LIST OF ILLUSTRATIONS--continued

ABSTRACT

An automated system has been designed and constructed to calibrate up to eight thermistors to within ±0.02°C for clinical applications. Calibrations are performed automatically, except for an initial instrumentation calibration which requires operator verification of accuracy.

An AIM-65 microcomputer is used along with a data acquisition and control interface and a 16-channel multiplexer, to establish a feedback controlled process which brings the temperature of a thermally shielded and insulated isothermal block into thermal equilibrium at specified calibration temperatures within the range 25-55°C. At each calibration point, the resistance, R, of each thermistor is measured and along with the temperature, T, of the standard thermistor. The coefficients of the Steinhart and Hart equation, $1/T(K) = A_0 + A_1 \mathrm{LnR} + A_2(\mathrm{LnR})^3$, for each thermistor are determined from a least squares fit of the resistance versus temperature data.

Twenty-four thermistors calibrated by this system were checked against a gallium melting-point cell at 29.773°C and a precision standard thermistor at 45.3°C. They were within ±0.02°C, except for two which were within ±0.03°C due to improper setup procedures. With planned modifications, the unit will be able to calibrate electronic thermometry systems with digital or analog outputs.

INTRODUCTION

Thermometers are available in many varieties, such as platinum resistance thermometers, thermistors, thermocouples or mercury-in-glass thermometers. Each type of thermometer is designed for specific applications. Some may have better temperature stability while others are inexpensive and convenient to use. The fundamental basis of thermometry has been reviewed by Compton and Quinn (1975) and recently by Hudson (1980), and a history of thermometers was described by Middleton (1966).

Platinum resistance thermometers and thermistors are resistance devices whereas thermocouples are thermoelectric junction devices. However, they are all electrical thermometers as compared to mercury-in-glass thermometers which operates on thermal expansion and they can be read directly without any instrumentation involved.

The standard platinum resistance thermometer (SPRT) is specified as the interpolating instrument on the International Pratical Temperature Scale of 1968 (IPTS-68), amended by H. Preston-Thomas (1976), for determining temperatures between the defined fixed points from 13.81 K to 903.89 K. Thermocouple sensors provide very small signals and minute inhomogeneities in the material of the leads are likely to provide spurious components in their outputs in the presence of thermal gradients adjacent to their active junctions (H. W. Trolander et al., 1977). As a result, it is difficult to achieve reproducibility in practical biological measurements to high orders of accuracy. Besides, their calibrations are highly dependent on the electronics in the reading devices. Thus the devices have to be calibrated. Thermistors can be made relatively small, they can be individually calibrated for high precision measurements. Their temperature and resistance characteristics are highly reproducible to better than 0.01°C.

Thermometers should be calibrated with a reliable, precision standard thermometer, on a universally accepted temperature scale. They should be checked periodically for temperature drifts in their calibrations as a result of aging or mishandling. Fixed-point temperatures, such as the ice-point or gallium melting-point (Sostman,1977; Sostman and Manley,1978) are excellent for this purpose.

Calibrating thermometers is very time consuming, especially when high accuracy is required. The average time spent in calibrating a set of four thermometers to 0.01°C manually, runs very close to ten hours. As a result of recent progress in technology, microcomputers have proved their value in many instrumentation and control applications. Therefore traditional thermometry calibration apparatuses can be replaced or upgraded by an automated micro-controller. Thermometers can be calibrated rather efficiently with an automated system, at a more cost-effective level without much reduction in reliability and performance.

This project involves the design and construction of an automated thermistor calibration system. It is specifically designed to calibrate clinical thermistors in either hypodermic needles or catheters. Thus a basic understanding of the various characteristics of thermistors is contingent to the design of this automated thermistor calibration system.

Thermistors are ceramic semiconductors. They are made from sintered mixtures of metallic oxides such as manganese, nickel, cobalt, copper, iron and uranium. The electrical resistance of a thermistor depends strongly on temperature. The high coefficients of resistance of thermistors, typically 3% to 5% per °C as compared to 0.4% per °C in platinum resistance thermometers, makes them ideal for sensing minute changes in temperature.

The electrical conductivity σ, of thermistors varies as $\exp(-Eg/2KT)$; where

Eg = the band gap energy of the semiconductor involved,

T = absolute temperature of the thermistor in kelvins, and

K = Boltzmann's Constant.

The temperature and resistance relationship of a thermistor can be represented by $1/T = A_0 + A_1(LnR)$, where R is the resistance of the thermistor, and A_0 and A_1 are constants characterizing individual thermistors. As described by J.S. Steinhart and S.R. Hart (1968), a third order term can be introduced to account for the non-linearities of thermistors. Thus the thermistor equation becomes $1/T = A_0 + A_1(LnR) + A_2(LnR)^3$, which has better than 0.01°C accuracy between 20°C and 60°C (Trolander et al., 1971).

The biological applications of electrical thermometers was described by H.W. Trolander (1971) and thermistor thermometry described by Kimball and Harraff(1971). The resistance versus temperature characteristics of thermistors may drift as a result of aging and mishandling. An investigation by S.D. Wood et al (1977) indicated that the stability of thermistors depends highly on their resistances and aging temperatures. After aging, the temperature characteristics of the thermistor may still vary, approximately a few millidegrees per year. However, if it continues to drift indefinitely, which implies that repeated recalibrations are necessary to retain accuracy.

In the past few years, we have been able to calibrate thermistors to better than 0.01°C accuracy without much complicated instrumentation (T.C. Cetas and W.G. Connor, 1978). Since only 0.1°C accuracy is required in hyperthemia applications, a microcomputer can be used to perform the same task more efficiently with at least 0.05°C accuracy.

Our automated thermistor calibration system can calibrate eight thermistors with an accuracy of 0.025°C or better, within the range 25°C to 55°C. Other than the initial instrumentation calibration and setups, the entire calibration process is fully controlled by the system itself and the data is recorded automatically. Therefore the system can be left totally unattended throughout the calibration process. Furthermore, it is designed with the possibility of calibrating other electronic thermometers with only minor modifications.

This thesis consists of five chapters. Chapter two describes the techniques we have been using to calibrate thermistors manually with an isothermal calibration block, a water-bath, a constant current source and a digital voltmeter. Then chapter two discusses some of the errors normally encountered in a typical calibration and a brief description of the basic requirements of an automated thermistor calibration system. Chapter three describes the design and construction of the calibration block used in this automated thermistor calibration system. It also discusses some of the thermal aspects of the different sections of this calibration block. Chapter four explains the electronic hardware involved and interfacing requirements of the different modules involved in this system. Chapter five explains the software required to perform the various computational and control tasks. Finally, chapter six presents the results obtained from the different testings followed by a description of some of the improvements that can be done to consolidate this unit to a better version and perhaps making duplicates at a less cost.

CALIBRATING THERMISTORS

In order for thermometers to read accurately, they must be well calibrated. The accuracy of a calibration depends highly on the temperature stability of the standard thermometer and the precision of the instruments involved. It is extremely important that all instrumemts are precisely calibrated, otherwise thermometry would be meaningless.

The resistance of a thermistor is a function of its temperature. If the thermistor is calibrated, its temperature can be determined readily by its characteristic equation (Steinhart and Hart, 1968) : $1/T = A_0 + A_1(LnR) + A_2(LnR)^3$. This resistance versus temperature characteristics can be determined in an isothermal calibration block by comparison with a standard thermometer. The constants A_0, A_1 and A_2 for each thermistor are determined by a least squares fit of the resistance versus temperature calibration data of the expression above.

Calibration Techniques

Presently, our thermistors are calibrated in an isothermal calibration block immersed in a temperature-controlled water-bath as described by Cetas and Connor (1978). The temperature of the calibration block is monitored by a standard thermistor(Series S-10, Thermometrics Inc.), its resistance is determined with a constant current source and a 5-1/2-digit digital voltmeter. Digital thermometers and chart recorders also are used to establish the temperature stability of the calibration block and the temperature of an outer bath relative to that of the calibration block so that reliable temperature measurements can be ensured.

The standard thermistor has been very carefully manufactured, aged and calibrated by the manufacturer against a standard platinum resistance thermometer from the National Bureau of Standards. It has a four-lead configuration and is sealed in a stainless steel sheath which further protects it from harsh environmental conditions.

The calibration block consists of two concentric cylinders as shown in figure (1). The outer block is made of a thin wall aluminum cylinder and the inner block is made of a solid cylinder of high purity aluminum. Due to the high thermal conductivity and specific heat of aluminum as well as the geometry of the calibration block, the temperature variation within the inner block is less than 0.005°C while the water-bath may vary as much as 0.5°C. The temperature fluctuations of the bath are attenuated by the long thermal time constant of the massive inner block and the high thermal impedance of the air coupling to the bath. Furthermore, the main heat flow is along the central aluminum rod. When the bath stabilizes, the block comes to average temperature of the bath and no significant gradient can exist so that thermometers are all in equilibrium at the same temperature.

The temperature stability of this calibration block and the resistances of the thermistors to be calibrated, are determined by applying a constant current of 10 μA to the thermistors all wired in series and by monitoring the potential across them. As the calibration

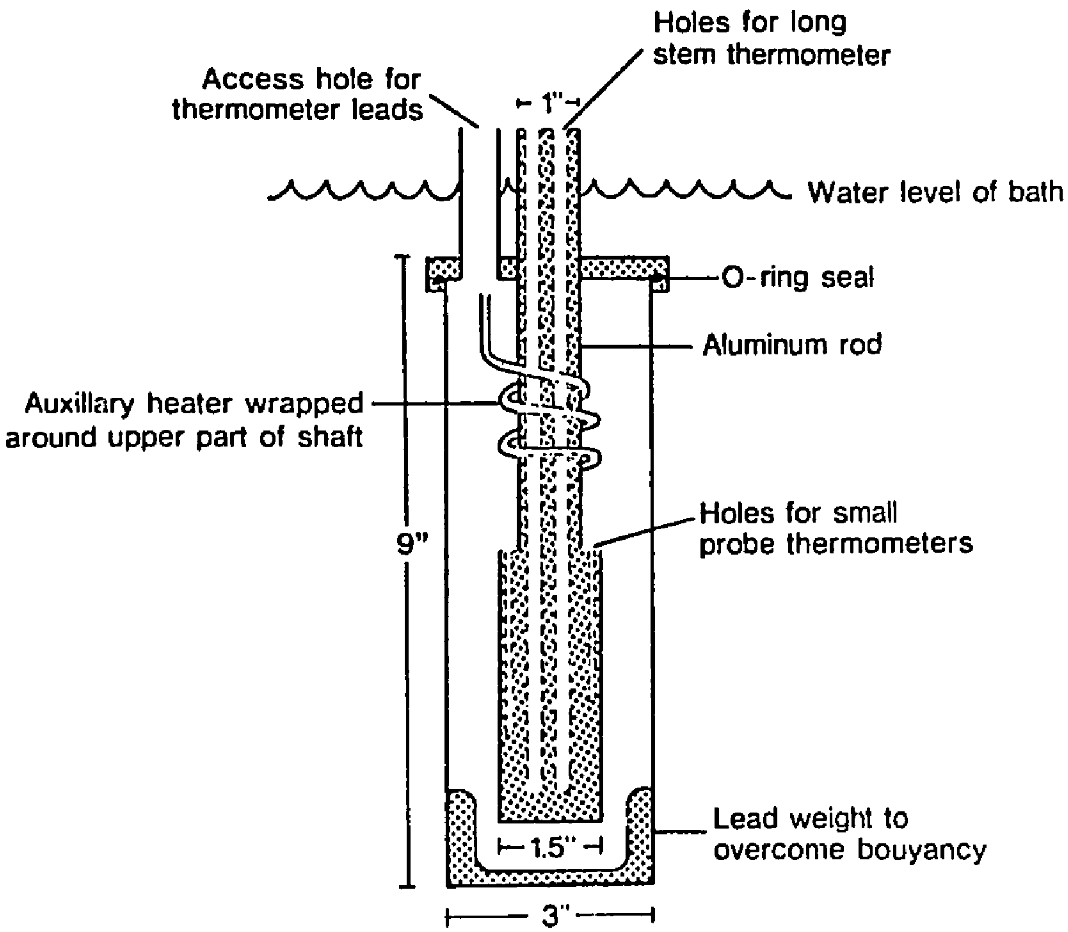

Figure (1). The calibration block described by Cetas and Connor (1978).

block approaches thermal equilibrium, the potential across the standard thermistor gradually approaches a constant. Thus the temperature stability of the calibration block is indicated by a steady voltage across the standard thermometer. When this signal reaches a plateau on the chart recorder, the voltages of all the thermistors are recorded, their resistances are calculated, and their temperatures are determined from the standard thermometer. Five to eight calibration points are necessary to determine the coefficients in the Steinhart and Hart equation (1968), $1/T(k) = A_0 + A_1(\mathrm{LnR}) + A_3(\mathrm{LnR})^3$, with a least squares fit which minimizes the square of the error between the data obtained in a calibration and and the Steinhart and Hart equation. Due to the uncertainty in instrumentation and some of the errors described below, five to eight data points provide better confidence in the calibration than the three required by a three constant expression. The results of a typical calibration is shown in Appendix A.

Error Analysis

The various sources of errors in a calibration are:

1. thermal gradients as a result of improper setups,
2. noise pickup in cables,
3. thermally generated EMFs,
4. instrumentation difficulties due to self-heating,
5. digital round-offs,
6. drifts in the standard thermometer.

In order to minimize the amount of error induced as a result of carelessness in setups, a routine calibration procedure has been followed. Thermal leakages along the thermistor leads are minimized by anchoring them to the block before they make contact with the ambient, so that thermal gradients along these leads can be reduced. Noise and RF interference can be reduced greatly by using shielded cables and separating RF and high voltage lines from low level signal lines. Filters should be incorporated whenever it is necessary although the noise rejection characteristics of our digital voltmeter precluded the need for additional filtering. Thermal EMFs are eliminated from resistance measurements by using current reversal techniques as shown in figure (2).

As a result of the small size of thermistors, only a limited amount of sensing current, I, can be used by these devices without causing self-heating (I^2R) which can cause inaccuracy in the measurements. On the other hand, as the sensing current is lowered, the voltages across the thermistors are decreased. Thus the resolution of the voltmeter must be increased. Typically for a thermistor of 2K Ω nominal resistance at 25°C and a 10 μA sensing current, 10 μV resolution is required to obtain 0.01°C accuracy.

In the curve fitting process, round-off errors that propagate through the computations can cause significant uncertainty in the fit. All computations should carry at least 12 significant digits of accuracy, except logarithm terms which carry 7 significant digits (see chapter five, Natural logarithm). Furthermore the raw data must be checked for obvious errors indicated by the measurements, especially when only a few data points are available.

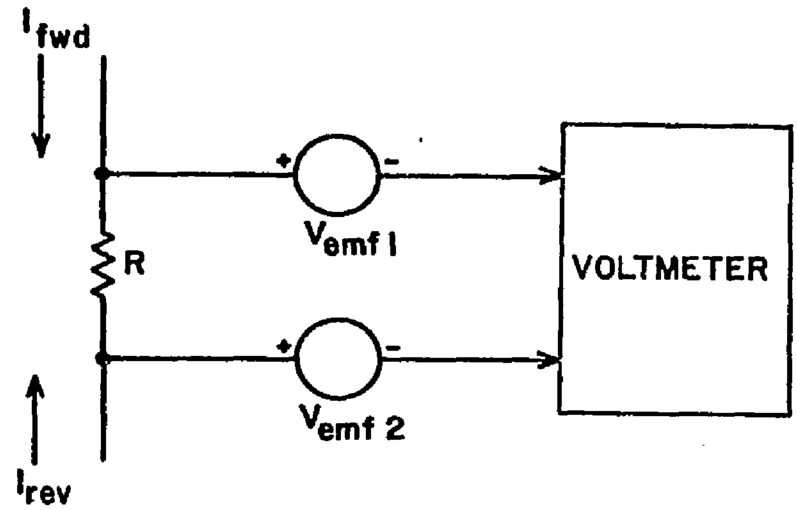

$$|I| = I_{fwd} = I_{rev}$$

$$V_{fwd} = V_{emf1} + V_{emf2} + IR$$
$$V_{rev} = V_{emf1} + V_{emf2} - IR$$

$$V = (V_{fwd} - V_{rev}) \div 2 = IR$$

Figure (2). Current reversal technique.

Lastly, the calibrations of the standard thermometer have been checked periodically with reliable sources to ensure the accuracy of all calibrations. A direct ice-point check is the simplest and we have observed the stability of our standard thermistor with this method over five years. Also checking the calibrated thermistors against a gallium cell at its melting-point (29.771°C) has served the dual purposes of checking the calibrated thermistors directly as well as indirectly verifying the stability of the standard thermistor.

The Basic Requirements of An Automated Thermistor Calibration System

The design of this automated thermistor calibration system consists of three main sections - the calibration block, the data acquisition and control interface (DACI) and the choice of an appropriate microcomputer.

In order to automate this system, the calibration block was designed to be interfaced to the computer through the DACI. The basic principles in its design remain the same as those used in the previous system (Cetas and Connor, 1978). In order to increase the thermal time constants between the inner and outer block cylinders and to reduce the overall size of this calibration block, the water-bath used in the earlier system was eliminated. Computer interfacing was implemented easily by using heating elements to control the temperatures of the inner and outer block cylinders directly. Furthermore, by eliminating the water-bath in favor of an outer electrically controlled cylinder, the power required to maintain the block at the various set temperatures is reduced and the system could be compactly constructed.

The procedures and software involved in controlling the calibration process depend very much on the structure of the microcomputer and its input/output (I/O) capabilities. Software development tools such as editor and assembler as well as flexible I/O functions for control applications should be available in that computer. Moreover, efficient non-volatile data storage is essential both for software development and for the storage of calibration results. Therefore a floppy disk unit was incorporated in the development prototype.

The requirements for the data acquisition and control interface (DACI) and its various functions can be determined by the design of the calibration block, the structure of the microcomputer and the intended performance of this calibration system. An accuracy of 0.1°C is required for the applications in clinical hyperthermia. Nevertheless, to have an adequate margin of error to insure that temperature measurements are within biological uncertainties, we decided to calibrate thermometers to at least 0.02°C. Thus the various data acquisition and temperature control components should provide better than 0.01°C resolution. Based on the results obtained from calibration apparatuses used presently, the analog-to-digital converter (A/D) must have a resolution of at least 10 μV in order for this system to resolve 0.01°C. High speed A/D is not necessary because the temperature variations within the calibration block are rather slow, due to the long intrinsic thermal time constants of the block cylinders. According to the thermal requirements of the calibration block, 8-bit digital-to-analog converters (D/A) with +10V outputs should satisfy the requirements in temperature control. Furthermore a channel multiplexer with enough channels for both data acquisition and temperature control is required. Other design considerations include the system power supplies and the mounting of the various components.

In order for this system to perform calibrations, software control is required for the feedback path provided by the data acquisition and temperature control components. Routines were developed to control the operation of the various devices and components. High precision computation algorithms are required to perform the calculations during the calibration process.

THE DESIGN AND CONSTRUCTION OF THE CALIBRATION BLOCK

The calibration block consists of an inner block cylinder, an outer cylinder, two sets of heating elements and a cooling coil as shown in figure (3). The outer cylinder is surrounded by high density insulation foam contained within a 5"x5"x5" metal box. The standard thermometer used in this system is a very stable thermistor placed along the axis of the inner block and at the same level as the the probes to be calibrated. The uncalibrated thermistors are inserted from the top into the eight holes arranged radially in the inner block as shown in figure (4).

In order to maintain the high accuracy required in this thermistor calibration system, many factors were considered in the design of the calibration block. Thermal leakages and gradients (between the inner and outer block, along the thermistor leads or between the block and the ambient), depend mostly on the geometry and construction of the block cylinders. Thermal resistances are affected mainly by the sizes of the block cylinders and the thermal conductivities of the materials used. Thermal gradients within the inner block cylinder where the thermistors are located, between the block cylinders, from the outer block to the ambient and due to heat flow within the calibration block itself should all be minimized in the design.

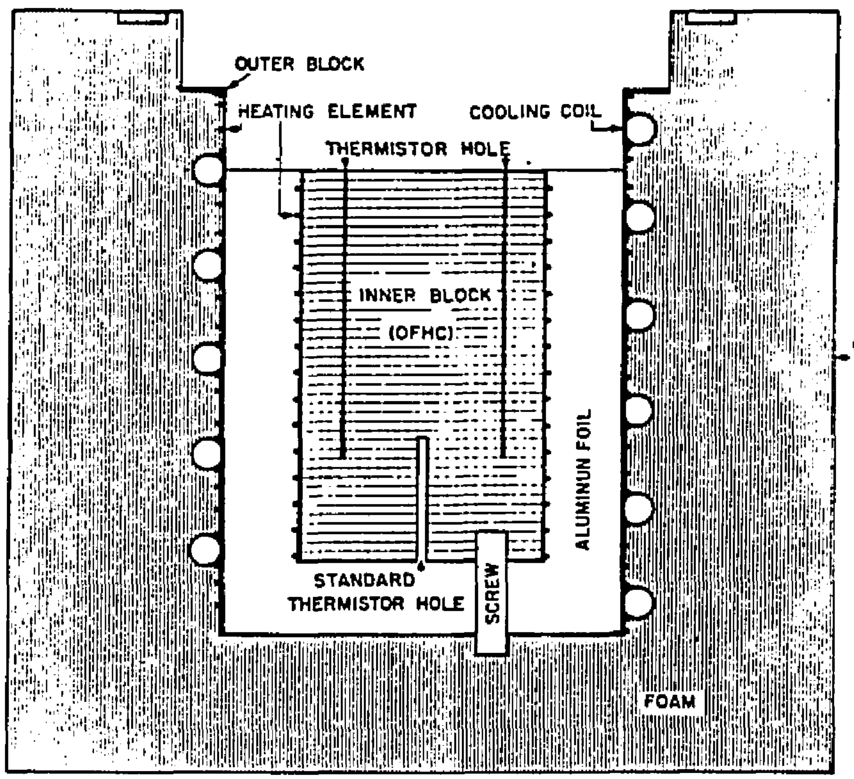

Figure (3). The calibration block used in this automatic calibration system.

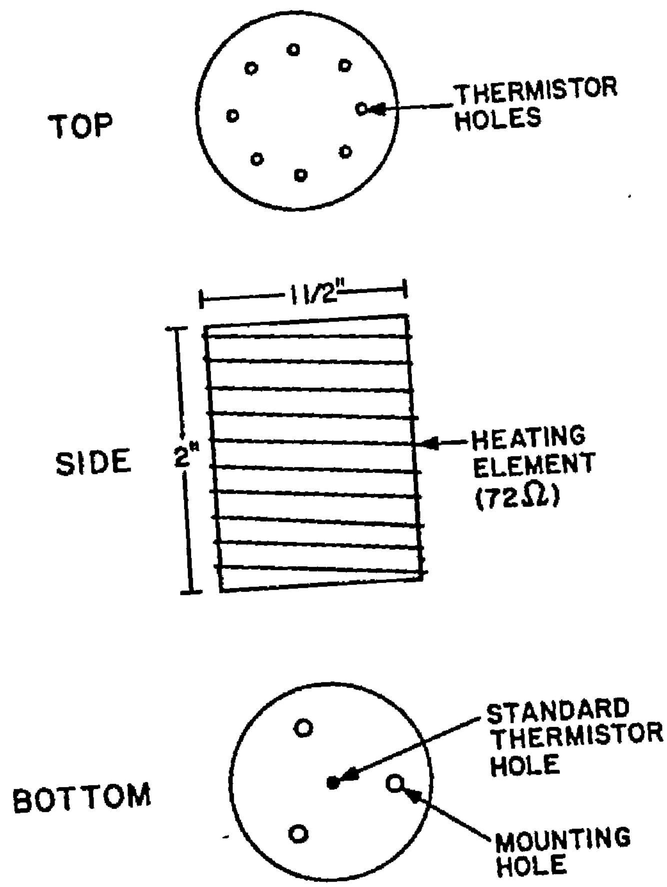

Figure (4). The inner block cylinder.

The inner block cylinder is made of oxygen-free hydrogenized copper (OFHC) which has high thermal conductivity (approximately 3.9 watts/cm °C at 300 K). This will reduce the thermal time constants and the thermal gradients within the inner block. Brass screws support the inner cylinder within the outer block so that the thermal gradients between the two block cylinders can be reduced. The thermal conductivity of brass is approximately 1/3 that of copper. The brass screws provide rather high thermal resistance to heat flow between the two block cylinders, but allows some heat conduction.

The outer cylinder consists of an 1/8"-wall copper cylinder, which has an 1/8" thick copper end cap soldered to the bottom. A removable thermal copper shunt plate covers the top. A five-turn, 1/4" O.D. copper cooling coil is soldered to the outer wall. The inner block is supported on the copper end cap by the brass screws. The thermal shunt plate mates with a 1/4" flange at the top of the outer block. This plate provides a low thermal resistance path to heat flow at the top of the outer block cylinder. Thus the temperature variations at the top of the calibration block, especially around the lid are reduced. The plate also acts as a heat-sink for the thermistor leads as shown in figure (5). There ia an insulated lid at the top of the block assembly, when it is fastened against its mounting, the thermistor leads are clamped against the copper shunt plate bringing them close to the temperature of the outer copper cylinder.

The cooling coil is connected to a thermoelectric cooling unit through a reservoir and a fluid pump as shown in the block diagram in

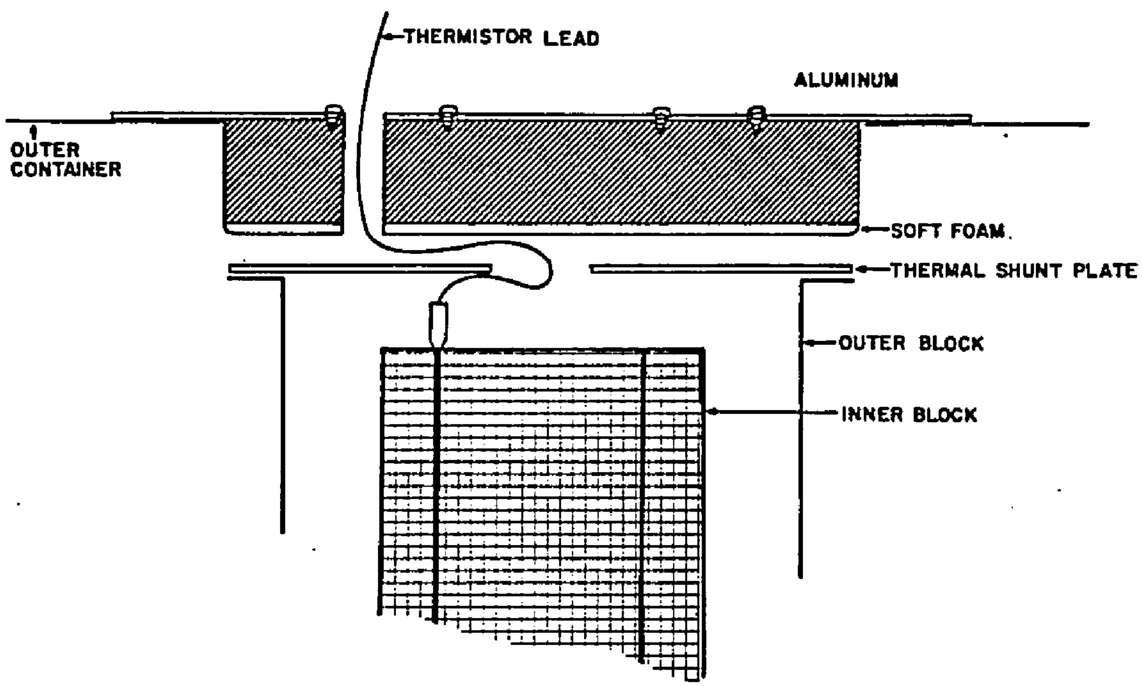

Figure (5). The thermal shunt plate as a heat-sink to the thermistor leads.

figure (6). This allows the calibration block to be cooled below ambient so that calibrations can be started at temperatures as low as 15°C. However, we intended that the thermoelectric cooler would permit fast cooling back to a low starting temperature so that subsequent runs could be started more quickly. Nevertheless, in practice, this unit did not work well due to the fact that the thermoelectric heat pump produces excessive heat within the cabinetry which, in turn increased the heat load on the block system and upset the thermal environment of the microprocessor and associated electronics. A simple design using circulating tap water controlled by a needle valve presumably would work better.

The heating elements for both block cylinders are made of non-inductively wound low resistance heater wires of 40 Ω /m resistivity. The inner and outer heating elements on the surface of the block cylinders have resistances of 50 Ω and 72 Ω respectively. They are wound at 0.65cm spacings and held in place with a thin layer of silicone rubber. All requred signal lines are brought to a 25 pin connector, mounted on the outer container. The calibration unit thus is separable as a stand alone module and interfacing and wiring difficulties can be greatly reduced.

In order to minimize the heat loss to the ambient, high density ureathane foam is used for insulation in the space between the outer container and the block cylinders. This insulating foam has a very low thermal conductivity and has sufficient rigidity to support the block cylinders. According to the Fourier Law of heat conduction,

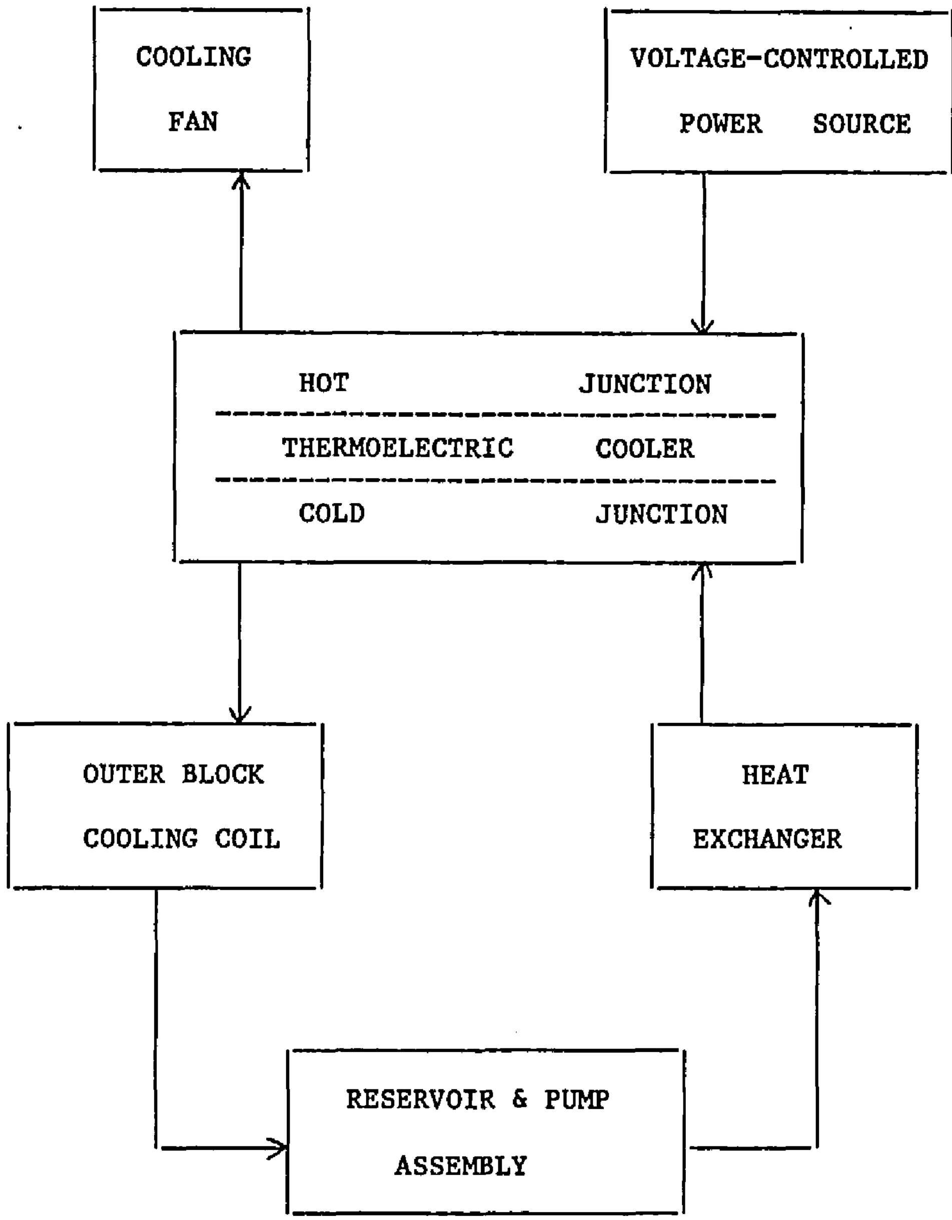

Figure (6). A block diagram of the thermoelectric cooling unit.

the heat, $\dot{Q}$, conducted through the foam is given by $\dot{Q} = \int K(\partial T/\partial x).\partial A$

where A = the cross-sectional area of heat conduction,

$\partial T/\partial x$ = the temperature gradient in the foam,

K = the thermal conductivity of the foam (approximately 0.039 W m-1 K-1).

This can be approximated for simplicity by $\dot{Q} = KA(\Delta T/\Delta x)$. By subsituting $\Delta x = .03m$ and $A = 2\pi(.055m)(.13m)$ and assuming $T_{block} - T_{air} = 30°C$, $\dot{Q}$ is approximately 1.7 W ≈ 2 W, which is within the capability of the heating elements.

After some initial testing, we found that the thermal time constant between the two block cylinders was more than an hour which resulted in very long equilibration times. Thus, the space between the cylinders was filled with crushed aluminum foil to reduce the intrinsic thermal time constant. Crushed aluminum foil has a relatively higher thermal conductivity than air. Furthermore, its high heat capacity makes it into an auxillary heat reservoir which will attenuate most of the temperature variations induced by the temperature fluctuations on the outer block cylinder. The attenuation of thermal oscillations by the aluminum foil can be characterized in analogy to an electrical low-pass filter as shown in figure (7).

When the block cylinders are brought to thermal equilibrium, the temperature variation within the inner cylinder should be less than 0.01°C as compared to the accuracy of the system(0.02°C). Otherwise, temperature differences may exist between the thermistors and the standard thermometer. All uncalibrated thermistors are located at the

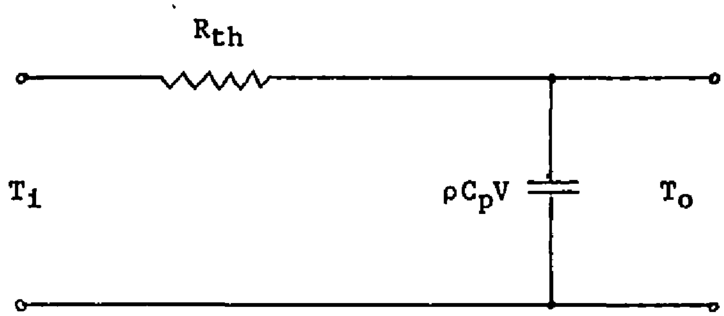

$T_o = T_i/R_{th}C_{th}\ (e^{-t/RthCth})$

t = time

R_{th} = thermal resistance

C_{th} = thermal capacitance

$Ln(r_i/r_o)/2\pi KL$ = thermal resistance of a hollowed cylinder

ρC_pV = thermal capacitance

where K = thermal conductivity of aluminum foil

ρ = density of aluminum foil

C_p = heat capacity of aluminum foil

V = volume of aluminum foil

r_i = inner radius of hollowed cylinder

r_o = outer radius of hollowed cylinder

L = length of cylinder

Figure (7). The low-pass filtering characteristics of thermal resistance and capacitance in the aluminum foil.

same radius on the inner block, therefore they are on the same isotherm. Thus the thermal gradients among these thermistors should be insignificant to the accuracy of their calibrations. Furthermore the temperature variation throughout the entire length of the inner block cylinder (measured at different depths with thermistors of known calibrations) is less than 0.005°C, and the vertical separation between the standard thermometer and the thermistors is less than 1/4". Thus the inaccuracy induced by this vertical separation is also insignificant to the results of the calibrations. At thermal equilibrium, the inner block is isothermal to better than 0.005°C as measured by the standard thermistor and thermistors attached to its outer surface during the various calibrations.

SYSTEM HARDWARE

The hardware involved in this calibration system consists of a microcomputer (AIM-65 from Rockwell International), an 8" floppy disk drive and controller, a 16-channel multiplexer, a data acquisition and control interface (DACI), a thermoelectric cooling unit and the power supplies for the various devices. In order to simplify the interface requirements within the system, the various components and devices selected must be highly compatible with each other. Furthermore, this system should be easy to operate and compact in its construction. A functional block diagram of this system is shown in figure (8). All the hardware data sheets are included in a supplement to this thesis : " An Automated Thermistor Calibration System - Hardware Specifications".

The Microcomputer - AIM-65

The AIM-65 is a 6502 microprocessor based single board microcomputer development system. It has a 20 character display, a 20 column thermal printer and an ASCII keyboard. System expansion and peripheral interfacing are accomplished through two input/output (I/O) buses, namely the expansion bus and the application bus. The expansion bus contains the data, address, control and clock signals of the system. The application bus includes two cassette I/O ports, a serial input, a teletype (TTY) output and two programmable 8-bit parallel I/O ports. The computer itself carries only 4 K-bytes of random access memory

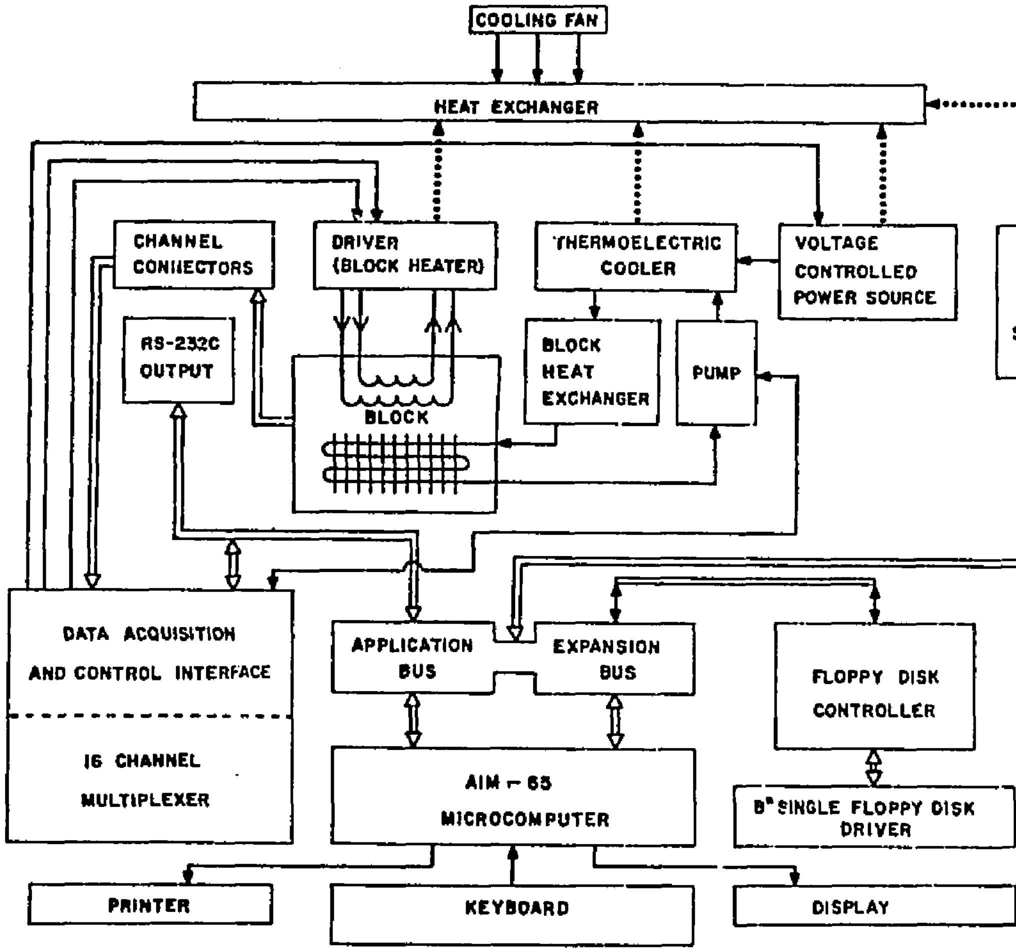

Figure (8). A functional block diagram of this automated thermistor calibration system.

(RAM); nevertheless it can accomodate 20 K-bytes of read only memory (ROM). The system requires 8 K-bytes of ROM for its internal operation. The remaining 12 K-bytes are available to store user programs. Alternatively, an optional assembler and Basic ROMs can be installed to enhance the programming flexibility of the system. The serial input and the TTY output have programmable baud rates of up to 2400 Baud. They can be modified easily with optical isolators or interface buffers to meet the RS-232C data transmission requirements.

Cassette data storage is rather slow and inconvenient, so an 8" floppy disk subsystem was incorporated to improve the non-volatile storage capabilities of this system. The floppy disk unit consists of a single-sided, single-density, 8" disk drive and a disk controller which has 16 K-bytes of RAM. The disk controller is fully compatible with the expansion bus on the AIM-65 and the disk drive was selected to be compatible with the requirements of the controller. Only 8 K-bytes of RAM are required by the controller for its direct memory access (DMA) transfers, leaving the other 8 K-bytes of RAM to be allocated to the AIM-65. This increases the user RAM on the AIM-65 to approximately 12 K-bytes. The manuals for the disk drive and controller should be consulted for details in their design, interface and operations.

The AIM-65 has a versatile interface adaptor (VIA) - 6522, which can be accessed through the application bus. It has two programmable 8-bit parallel I/O ports (port A and port B) with two programmable handshake lines per port (CA1, CA2, CB1 and CB2), two 16-bit timers and a shift register as shown in figure (9). Both the multiplexer and

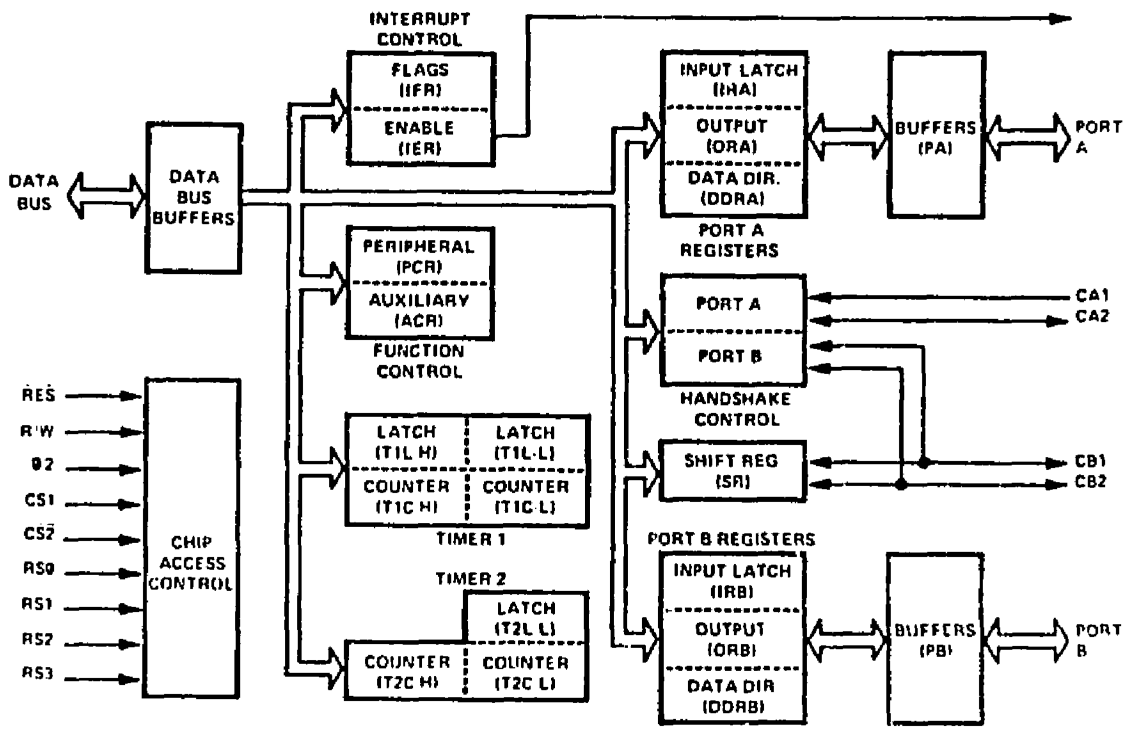

Figure (9). A block diagram of the 6522 VIA.

the DACI are connected to the AIM-65 through this VIA. The upper four bits of port A are programmed to input data from an A/D on the DACI, and the lower four bits are used to address the 16 channels on the multiplexer, whereas port B is programmed to ouput data to three D/As on the DACI. Thus the difficulties involved in interfacing is greatly reduced. The VIA - 6522 data sheets should be consulted for details in its timing and operation.

The channel multiplexer and the DACI must satisfy the power-on requirements on the application bus. During power-on, all of the I/O lines on the VIA are being reset as inputs by the system reset ($\overline{RES}$) from the 6502. Due to the internal active pullups in the VIA, all inputs connected to its I/O ports will have high level logic. In order to prevent power-on latch up problems, devices such as A/D, D/A or relays must be initialized to predefined states. The timing and gating of the various interfacing components at power-on must be considered carefully.

The 16-Channel Multiplexer

Figure (10) is a schematic diagram of the 16-channel multiplexer. It consists of a 4-to-16 decoder, eight hex buffers with high voltage outputs, a dual J-K flip-flop and 12 mercury-wetted switches. The decoder is a 74LS154 which is addressed by the lower 4 bits of port A. It has two enable inputs, one is grounded while the other one is connected to $\overline{CB2}$. Thus the decoder is enabled only when CB2 = "1". When the data at port A is unstable, this decoder must be disabled.

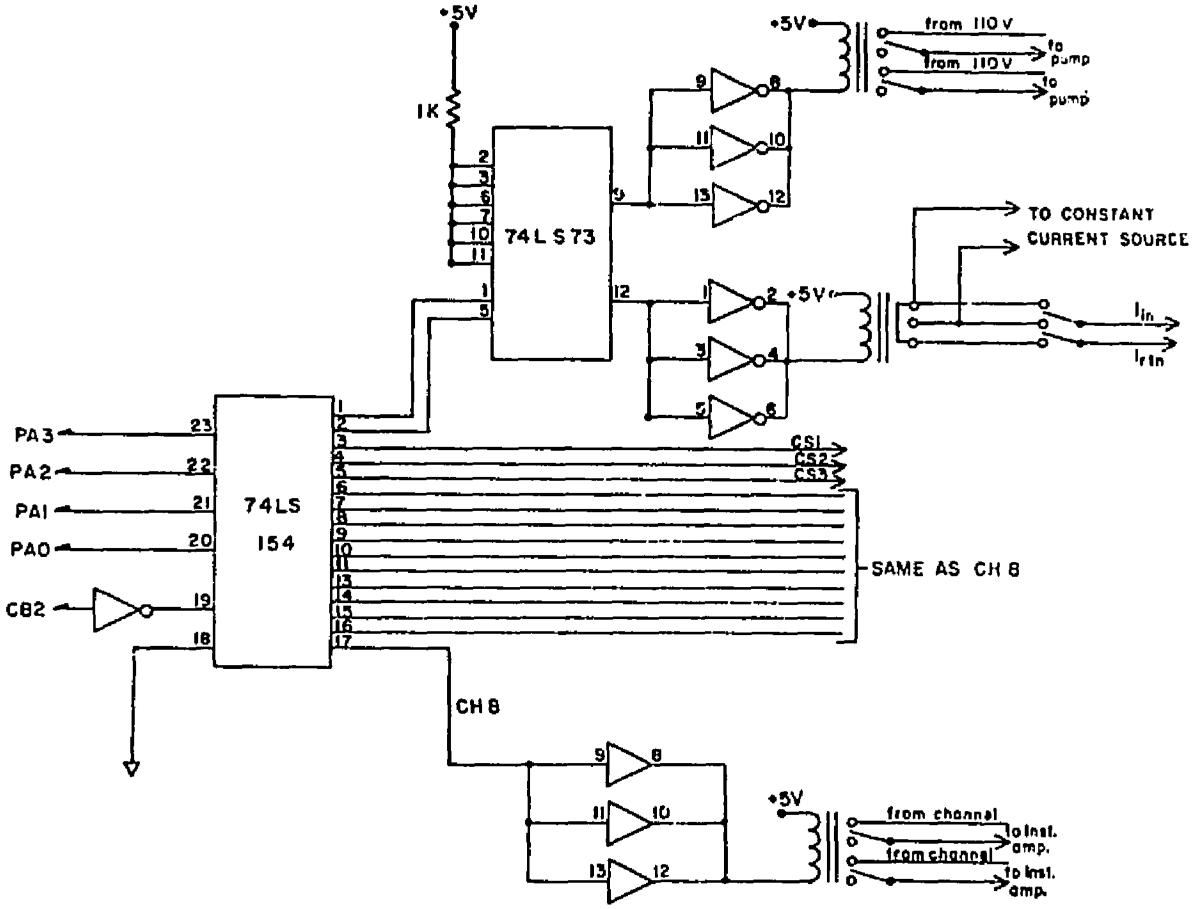

Figure (10). The circuit diagram of the 16-channel multiplexer interface.

Otherwise unstable addresses will produce glitches which will trigger a series of channels rather than specific channels.

Table (1) is a list of the thermistor channels and devices that are addressed by this multiplexer. Channel 3, 4 and 5 are used to enable the D/As on the DACI and channel 6 through 16 are connected to mercury-wetted switches. Each TTL buffer (7406/7407) can sink only 40 mA, but each mercury-wetted switch requires approximately 100 mA to operate. Consequently, three buffers are required to power each mercury-wetted switch.

The first two channels are used to control the current reversal operation and the on/off of the circulating pump for the thermoelectric cooling unit. Both of these channels are each doubly buffered by a J-K flip-flop (74LS73) and three buffers (same as the ones used for the mercury-wetted switches). By connecting the flip-flops in the toggle mode, the corresponding channels are activated or deactivated whenever they are addressed (if the channel is activated, then it will be deactivated or vice versa). Thus the current reversal switch can be preset to forward or reverse operation before the addressing of a thermistor channel and the pump can remain turned on or off while the other channels are actived.

During power-on, all the address lines of the decoder assume high logic due to active pullups at port A, channel 16 is activated and all other channels remain inactive. After power-on, this decoder must be initialized by first disabling it and then programming the

Table (1). The channel assignments of the multiplexer.

PA3	PA2	PA1	PA0	channel	device
Ø	Ø	Ø	Ø	1	current reversal switch
Ø	Ø	Ø	1	2	fluid pump relay
Ø	Ø	1	Ø	3	thermoelectric cooler D/A
Ø	Ø	1	1	4	inner block heater D/A
Ø	1	Ø	Ø	5	outer block heater D/A
Ø	1	Ø	1	6	1 K Ω resistor
Ø	1	1	Ø	7	standard thermistor
Ø	1	1	1	8	outer block sensing thermistor
1	Ø	Ø	Ø	9	thermistor channel # 1
1	Ø	Ø	1	10	thermistor channel # 2
1	Ø	1	Ø	11	thermistor channel # 3
1	Ø	1	1	12	thermistor channel # 4
1	1	Ø	Ø	13	thermistor channel # 5
1	1	Ø	1	14	thermistor channel # 6
1	1	1	Ø	15	thermistor channel # 7
1	1	1	1	16	thermistor channel # 8

lower four bits of port A as outputs. Otherwise this interface will remain at channel 16 indefinitely.

The Data Acquisition and Control Interface (DACI)

The major function of this interface is to allow the various analog and digital subsystems to communicate with each other so that feedback control can be established. This interface consists of a 5-1/2-digit A/D, three 8-bit D/As, an instrumentation amplifier, a constant current source and a 20 mA current loop to RS-232C buffer. Under the directions of the AIM-65, a sampled data feedback control process is established through the A/D and D/As.

The A/D

An integrating A/D with 4-1/2 digit accuracy and 5-1/2 digit resolution is used in this interface. It consists of the AD7555 ADC subsystem (Analog Devices, Inc.), a buffer, an integrator, a voltage comparator, a voltage reference and a frequency reference. The schematic diagram of this A/D is shown in figure (11).

The AD7555 is a monolithic CMOS, quad slope A/D subsystem. It contains most of the digital logic required for an A/D on a 28 pin chip. Its quad slope conversion algorithm is capable of converting the input drift errors of external amplifiers into a digital number and subsequently reducing the total system drift error to a second order effect. This ADC subsystem has a multiplexed BCD output that requires only four interfacing lines for 21 bits of data. Only four control lines are required for microcomputer control, namely SCC, $\overline{\text{DAV}}$,

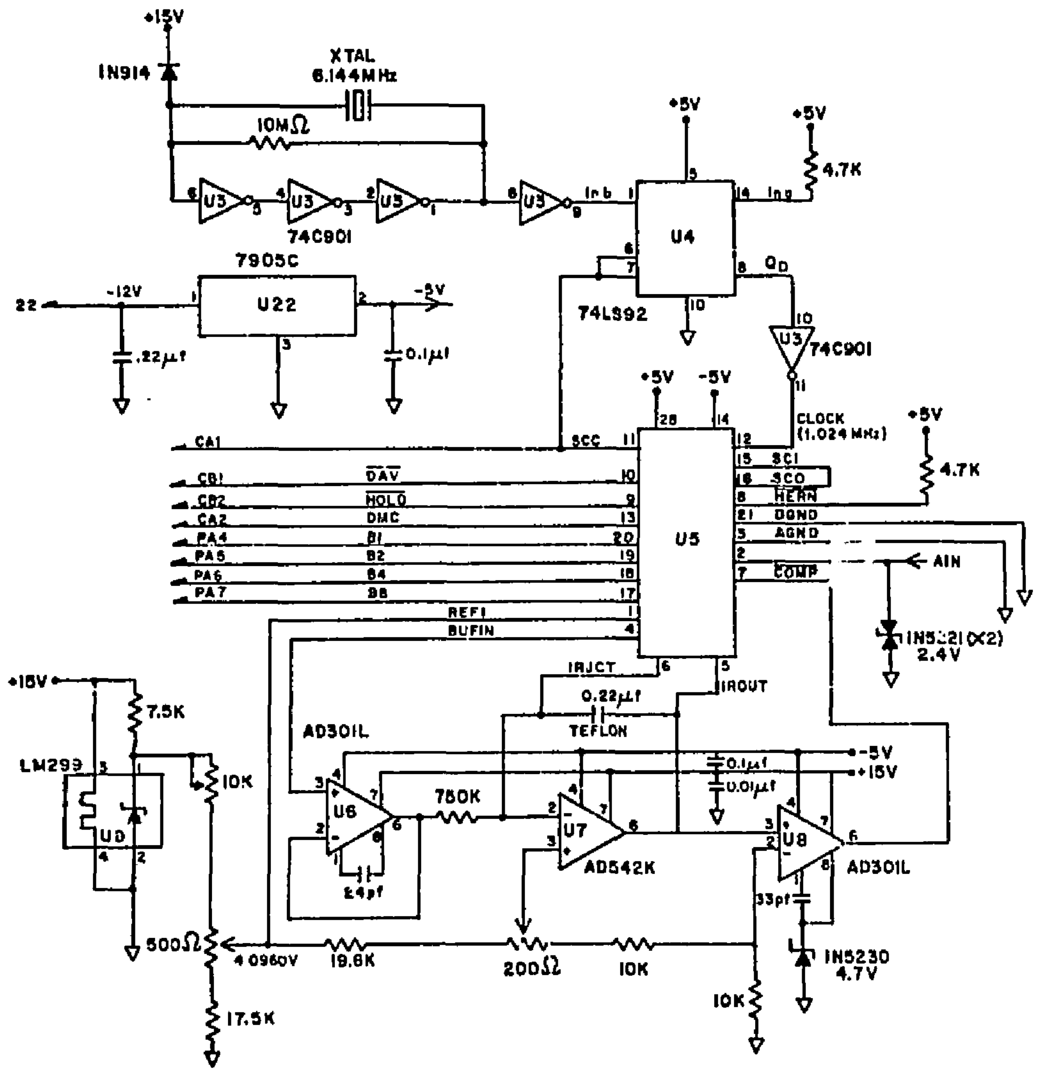

Figure (11). The circuit diagram of the A/D.

$\overline{\text{HOLD}}$ and DMC. Thus it can be easily interfaced to the AIM-65 through the application bus with its on-board VIA. The AD7555 data sheets should be consulted for details of the quad slope integrating algorithm.

This ADC subsystem has an input range of ± 2.0V. The BCD data outputs are connected to the upper four bits of port A and the control lines are connected to the handshake lines CA1, CA2, CB1 and CB2 as listed in table (2). The start of a conversion is initiated by a leading edge on DMC while $\overline{\text{HOLD}}$ is high, whereas the end of a conversion is indicated by a low to high transition on SCC. New data is transfered from the internal counters into the output latches of the AD 7555 by three DMC pulses. After the data is latched, a trailing edge on $\overline{\text{DAV}}$ indicates that more DMC pulses can be applied to update the latched data into the BCD buffer. Further conversions can be inhibited by lowering $\overline{\text{HOLD}}$ and the results can be read digit by digit into port A under the control of the DMC pulses on CB1. The data sheets of the AD7555 should be consulted for details of its interface and operations. The timing diagram for interfacing this A/D with the AIM-65 is shown in figure (12).

The integrator consists of a BI-FET op-amp (AD542KH, Analog Devices, Inc.), a 750K Ω low temperature coefficient resistor and a 0.22 μf low leakage and low dielectric absorption teflon type capacitor. The voltage reference required by the AD7555 uses a temperature stabilized zener reference (LM299H) which has a temperature coefficient of 0.0001% per °C and a long term stability of 20 ppm. Voltage dividers are used in providing the 4.0960V required by the AD7555 and the 2 V reference input for the voltage comparator. The 1.024 MHz frequency reference

Table (2). The interfacing signal assignment of the A/D
(refer to AD7555 and 6522 data sheets for signal definitions)

A/D AD7555	(pin)	AIM-65 application bus	(pin)
SCC	(11)	CA1	(20)
$\overline{\text{DAV}}$	(10)	CB1	(18)
$\overline{\text{HOLD}}$	(9)	CB2	(17)
DMC	(13)	CA2	(21)
B1	(20)	PA4	(13)
B2	(19)	PA5	(16)
B4	(18)	PA6	(17)
B8	(17)	PA7	(15)

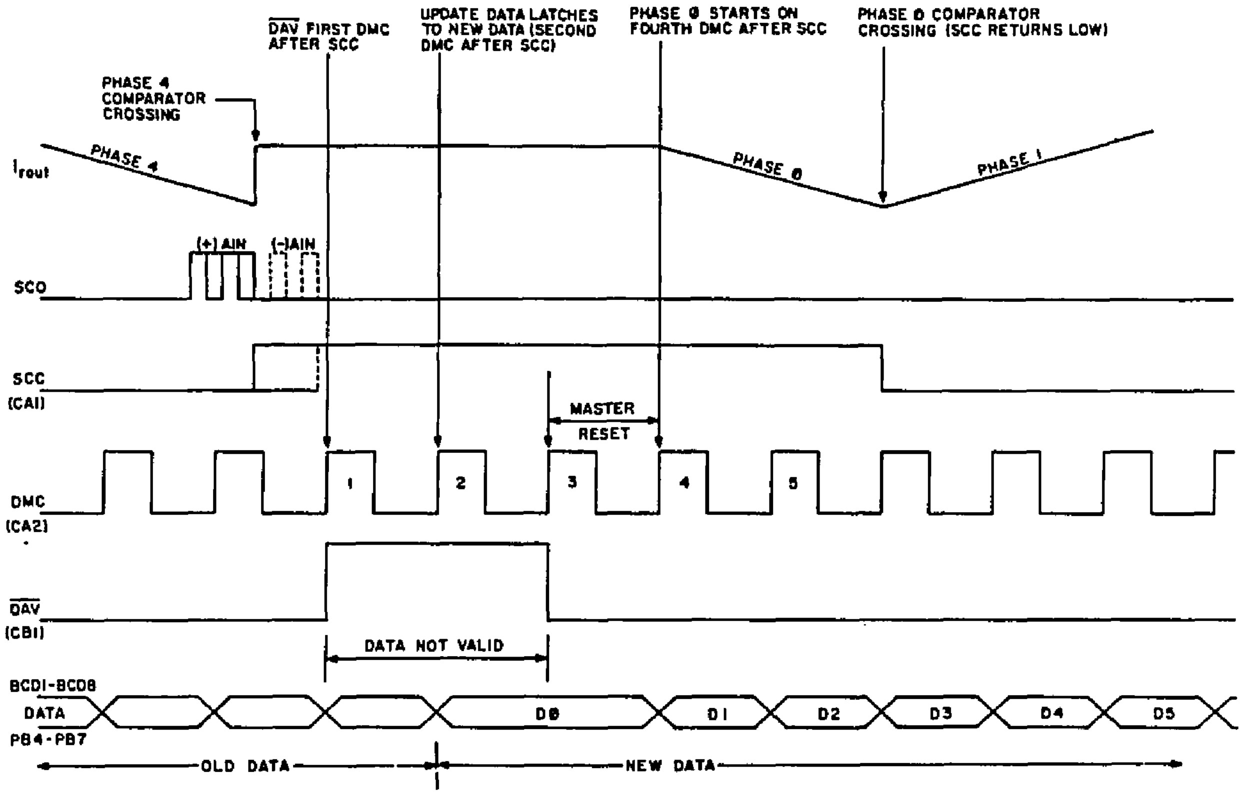

Figure (12). The timing diagram for interfacing the AD7555 to the AIM-65.

is obtained from a 6.144 MHz crystal-controlled oscillator and a divide-by-6 counter.

The timing of the four phases of the quad slope integrating algorithm (patented by Analog Devices, Inc.) is shown in figure (13). They are controlled by the various switches in the AD7555 and the zero-crossing of the voltage comparator. As a result of the quad slope algorithm, this voltage comparator always approaches the zero-crossing from the same direction, therefore hysteresis effects are eliminated.

The D/As

Three D/As (AD558) are incorporated into the DACI for controlling the heating elements in the block cylinders and the thermoelectric cooler. Figure (14) is the schematic diagram of the D/As and the corresponding interface circuitries. Two of the D/A outputs are connected to darlington drivers in a common emitter configuration, which provide the required power to the heaters in the calibration block. The other one is buffered by an op-amp which controls the current output of the power source to the thermoelectric cooler. In order to reduce the loading on port B, these D/As are buffered by a 74LS273 and data is latched into the corresponding D/A by the outputs of channels 3 - 5 on the 16-channel multiplexer. During power-on, all three D/As are enabled by $\overline{\text{RES}}$ and the outputs of the buffer are also cleared by $\overline{\text{RES}}$, thus zeroes are latched into the D/As. After the system reset sequence, whenever these channels are addressed, the data at port B is loaded into the

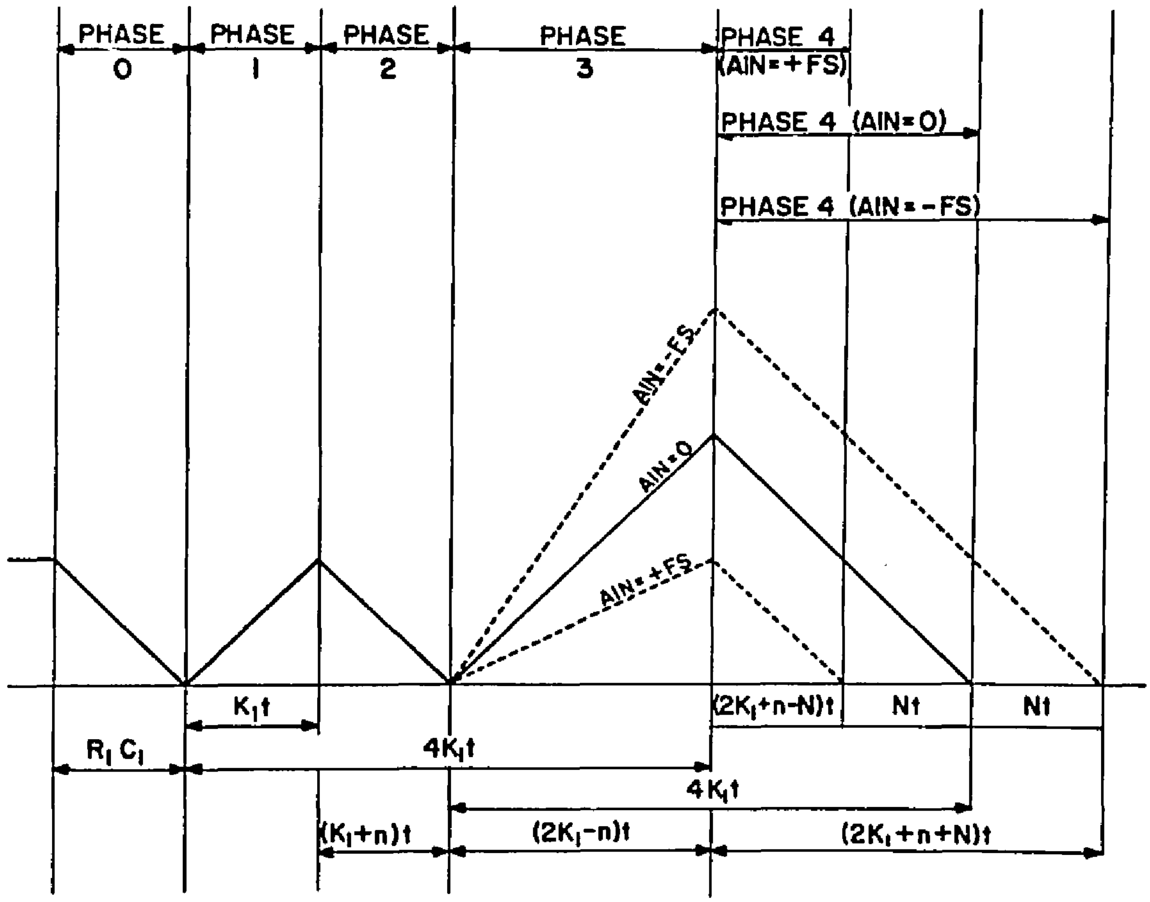

1. for 5-1/2 digit mode, K_1=102400, t = 2/1.024MHz.
2. n = error count due to amplifier offsets etc.
   (can be positive or negative).
3. N = number of counts at SCO corresponding to Ain.
4. Ain = analog input voltage.

Figure (13). The timing of the four phases of the quad slope integration (Analog Devices, Inc.).

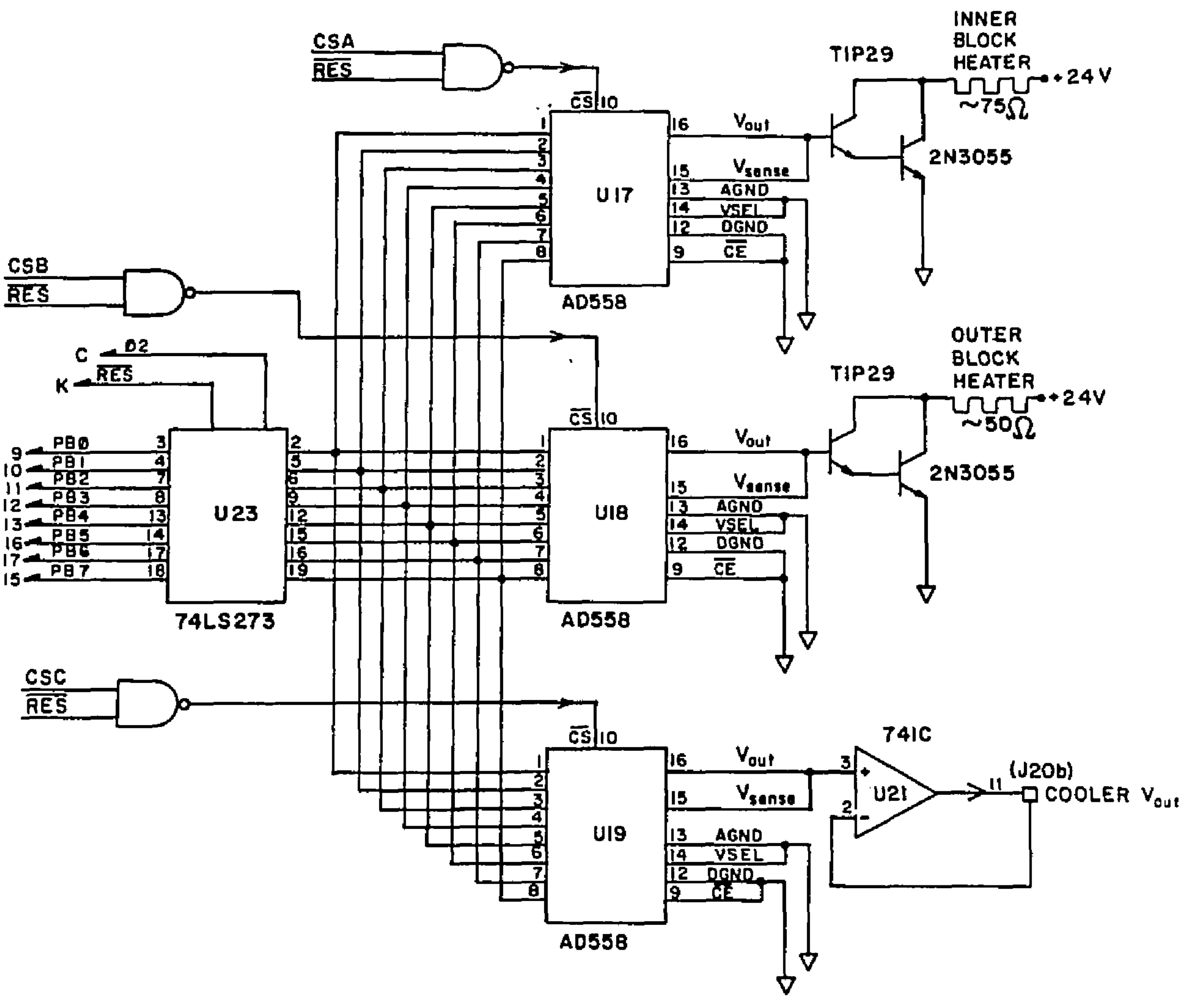

Figure (14). The circuit diagram of the D/As and their corresponding drivers.

corresponding D/A. As long as the channel remains active, the internal latches within the corresponding D/A will stay transparent to the data from port B. When the channel is deactivated, the data is latched instantaneously into the D/A. The timing diagram for interfacing the AD558 to port B is shown in figure (15).

Instrumentation amplifier, constant current source and RS-232C

The instrumentation amplifier is used mainly to convert the voltage across the thermistors into ground referenced voltages which can then be fed into the A/D. Besides, it also offers isolation between the channels and the A/D.

Figure (16) is a circuit diagram of the instrumentation amplifier and the connections of the thermistor channels. All the thermistors, including the standard thermistor, outer block sensing thermistor and the standard resistor are connected in series as shown in figure (16). In this way, the same amount of current from the constant current source is flowing through every thermistor. Thus, by reading the voltage of the standard resistor and the voltage of each thermistor channel, the resistance of each thermistor channel can be calculated by $(V_{ch}/V_{stdR})R_{std}$, where

V_{ch} = voltage read on thermistor channel

V_{stdR} = voltage read on the standard resistor channel, and

R_{std} = the resistance of the standard resistor (999.984 Ω)).

The resistance value of the standard resistor, 999.984 Ω, was determined with a Data Precision model 3500 digital voltmeter, a 10 μA

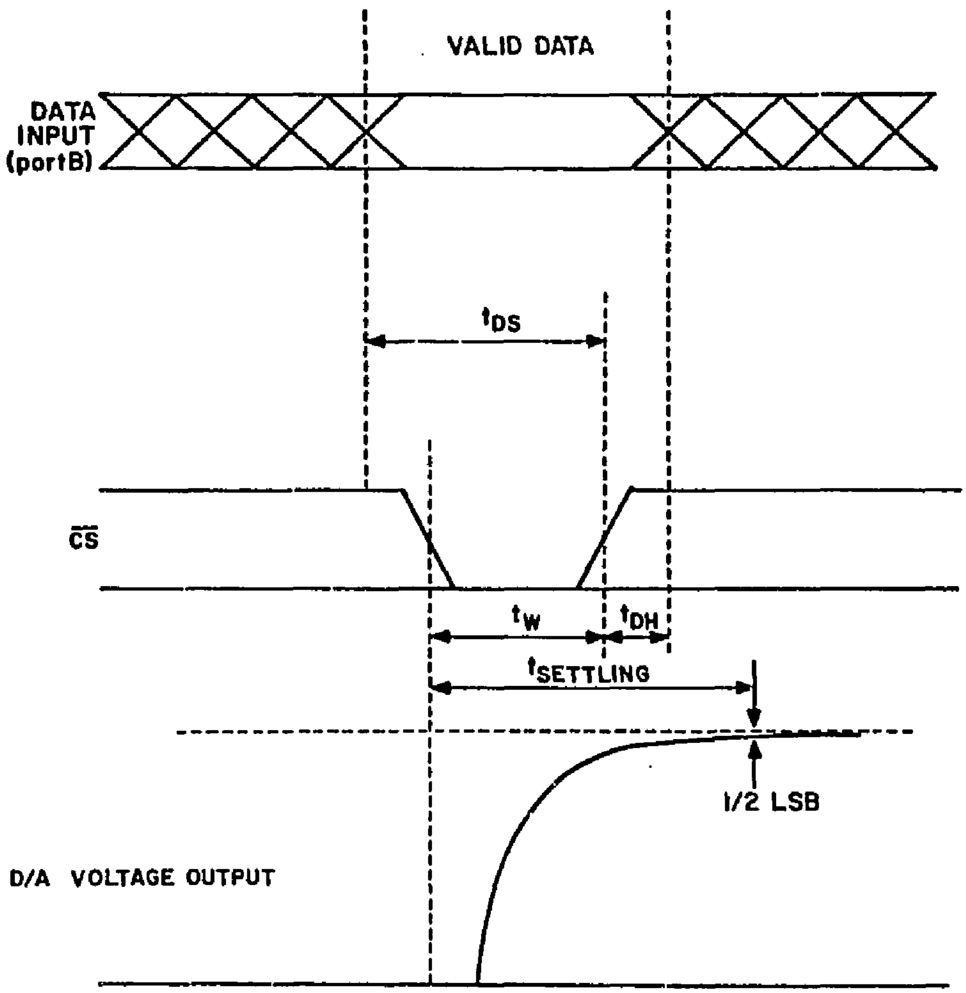

t_W (strobe pulse width) = 100 ns min.
t_{DH} (data hold time) = 10 ns max.
t_{DS} (data setup time) = 100 ns min.
$t_{settling}$ (output voltage settling time) = 3.0 µs max.

Figure (15). The timing diagram of the AD558.

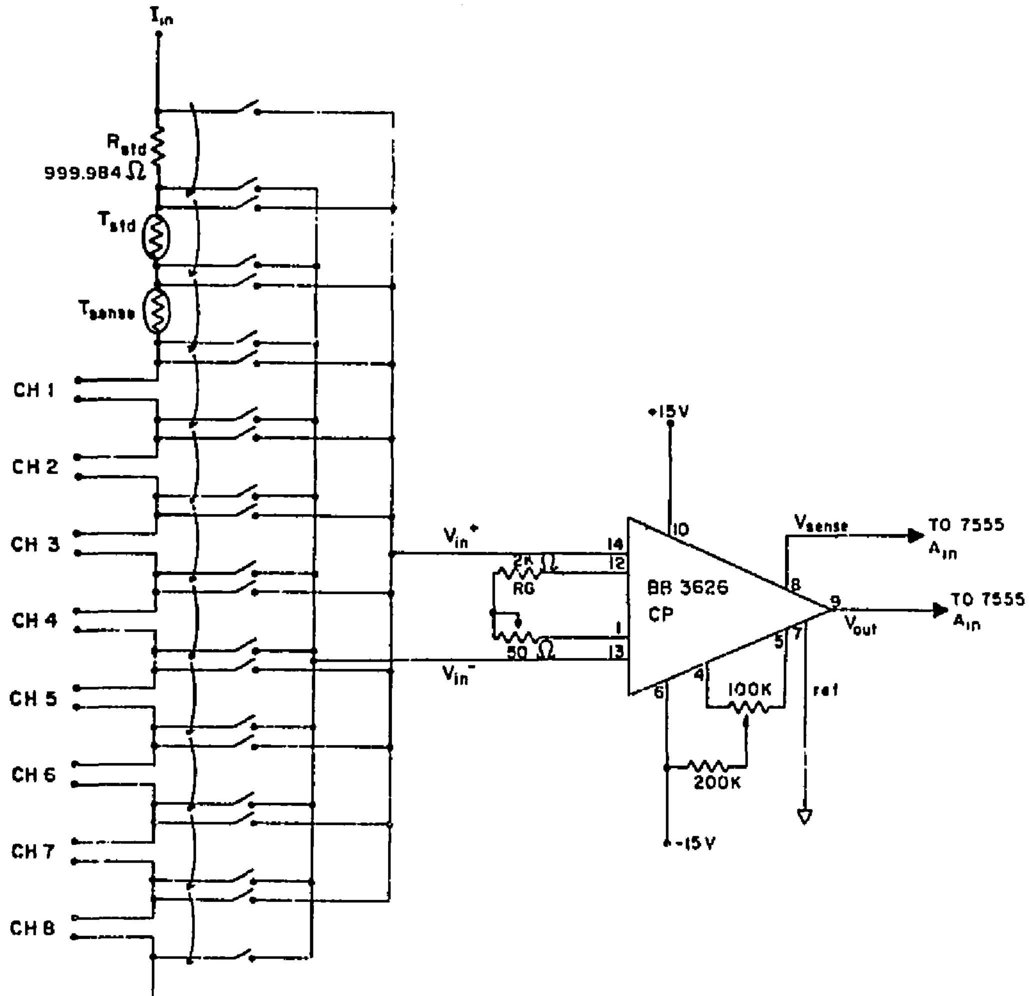

I_{in} and I_{rtn} are connected to the constant current soucre through the current reversal relay.

T_{std} = standard thermistor
T_{sense} = outer block sensing thermistor

Figure (16). the instrumentation amplifier and the connections of the thermistor channels.

constant current source and a 9999.86 Ω , 0.1% precision resistor. The resistance and temperature stability of this precision standard resistor had been certified by the manufacturer (Julie Research Laboratory Co.).

The constant current source consists of an op-amp (AD542KH) and a 6.95V buried zener reference. This op-amp provides a constant current to a floating load (the thermistor channels) in its feedback path. The current is adjusted by trimming the resistance of the 10 K Ω at the non-inverting input of this op-amp as shown in figure (17). This changes the voltage across the 3.3 K Ω resistor which in turn, adjusts the current accordingly.

The 20 mA current loop (TTY) output on the AIM-65 is converted to the RS-232C format through an optical isolator, 4N33 as shown in figure (18). Since the handshake lines CTS (clear to send) and RTS (request to send) are both terminated by pullups, and the data is not buffered on this serial I/O channel, the peripheral device should be set to the same baud rate as the AIM-65 for reliable data transfer.

The Thermoelectric Cooler

The thermoelectric cooler was installed to allow the calibration block to be cooled to ambient temperatures after a calibration so that subsequent calibration runs could be started. They are particalarly suited for automatic control applications with minimal circuitry involved. A thermoelectric cooler (Melcor,1980) is an array of cooling couples connected electrically in series and thermally in parallel as shown in figure (19). These cooling couples are made from elements of semiconductors,

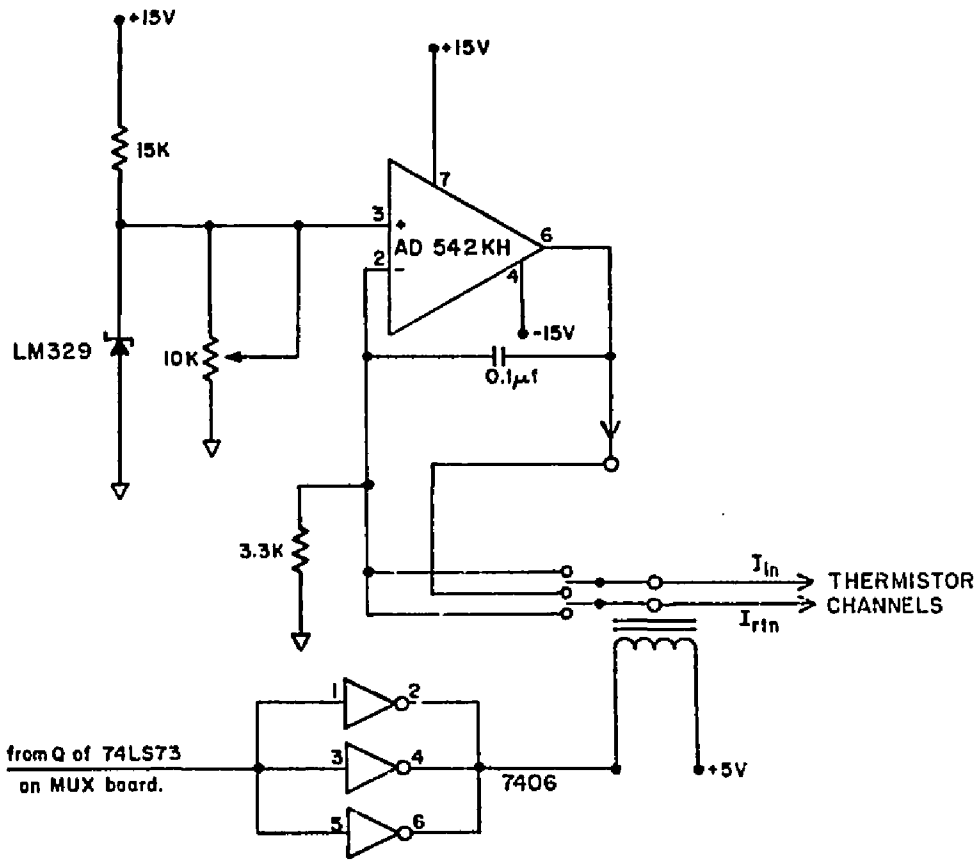

Figure (17). The constant current source.

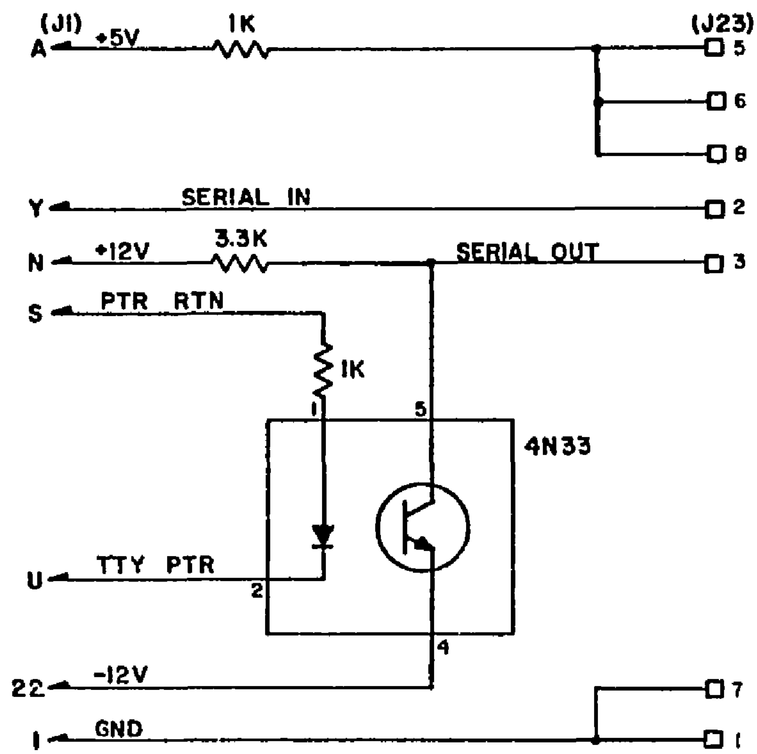

Figure (18). The current loop to RS-232C buffer.

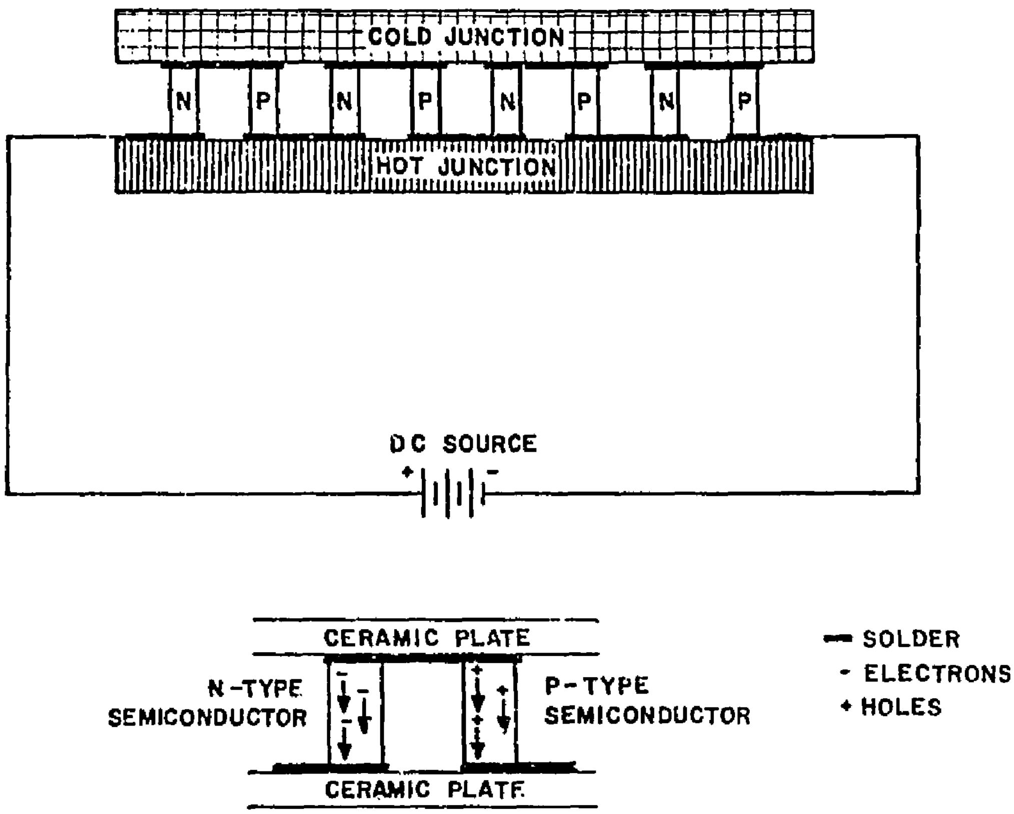

Figure (19). A thermoelectric cooling device (Melcor).

primarily bismuth telluride heavily doped to form the P-N junction. The rate of heat transfer from the cold junction to the hot junction is proportional to the number of cooling elements and the amount of current flowing through them. A typical voltage versus current characteristic curve for these devices (Melcor,1980) is shown in figure (20). Since the amount of power required by these devices depends on the operating points which are functions of the temperatures of the hot and cold junctions, an adequate heat-sink must be provided for the hot junction for efficient cooling to be achieved.

The thermoelectric cooler incorporated in this system consists of two 8 X 8 arrays of cooling couples. When the hot junctions are at approximately 38°C (measured), 4.5A is drawn and the final steady state temperature at the cold junction is approximately 15°C. However, due to the limited surface area at the cold junction and the inefficiency in the fluid circulation assembly, the calibration block itself can only be cooled to approximately 23°C. With the cold junction cooled to 15°C, the temperatures of the fluid are approximately 19°C at the cold junction heat exchanger, 22°C in the cooling coil (around the outer block) and 24 - 26°C at the pump outlet.

In order to achieve variable cooling rates, a voltage-controlled current source is used to power the thermoelectric cooling unit. The current output in this power source is controlled by a D/A through a buffer op-amp. By changing the inputs to the D/A, the amount of current can be adjusted accordingly. Figure (21) shows the input voltage to

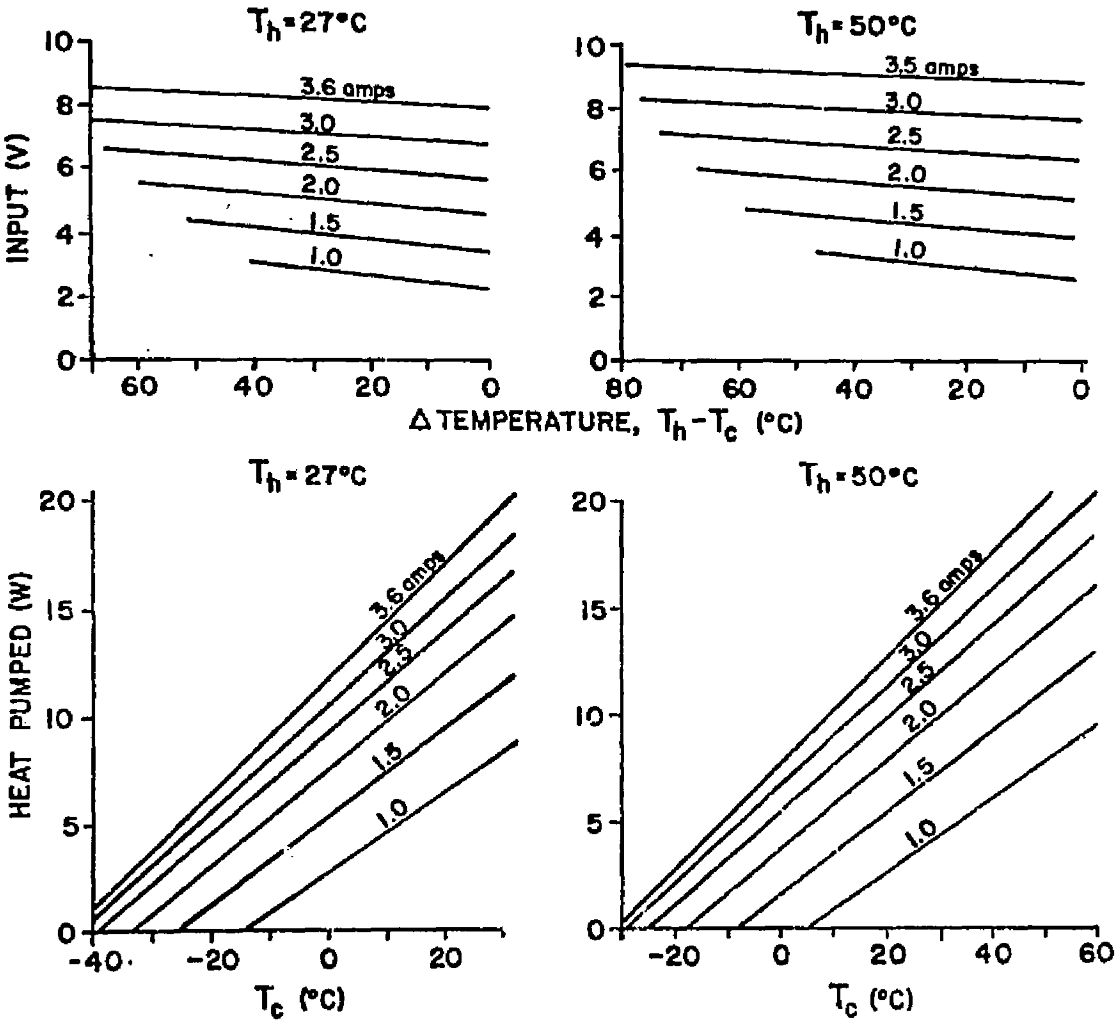

T_c = cold junction temperature
T_h = hot junction temperature

Figure (20). Typical voltage versus current characteristic curves of a thermoelectric cooling device (Melcor).

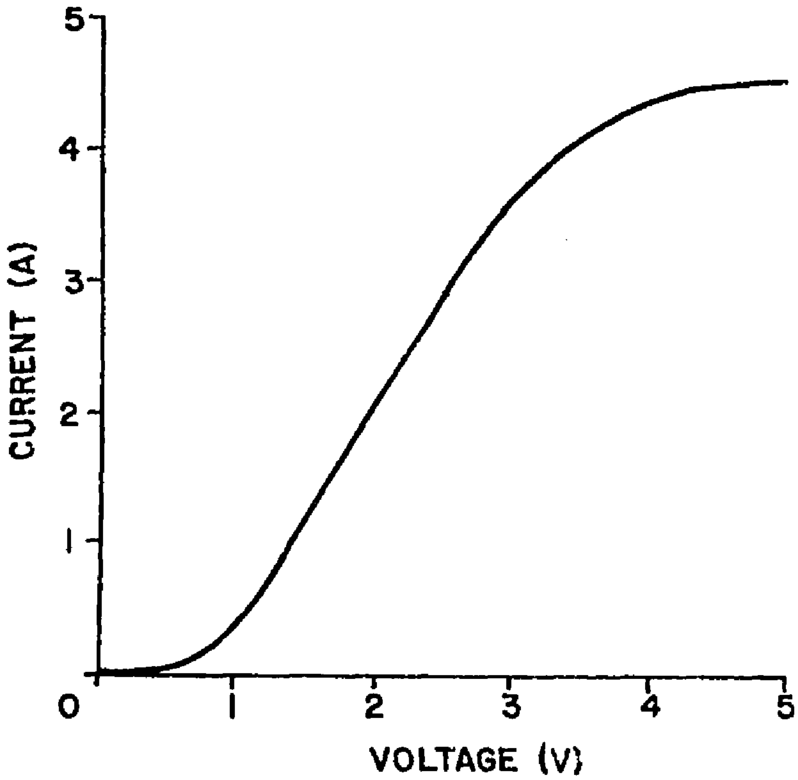

Figure (21). The voltage to current relationship of the thermoelectric cooler power supply.

output current relationship of this power source. The circuit diagram of this power supply is shown in figure (22).

System Power Sypplies

The power supply requirements for the various devices in the calibration system is summarized in table (3). The main A.C. input is filtered by a power line filter to reduce RF and noise pickup. The D.C. power required consists of six different voltages : +24V, +5V, ±15V and ±12V. The ±12V and ±15V are power supply modules whereas the +24V and +5V are designed around the 723 variable voltage regulators. The circuitries for the +5V and +24V power supplies are shown in figure (23). These power supplies are mounted towards the back of the system cabinet. They are isolated from the rest of the system by a bank of heat-sinks as shown in the physical layout of this system in figure (24). The amount of heat dissipated by the transformers and drivers are localized and forced air cooling can be concentrated on this particular section of the system. Thus the temperatures of the various electronic modules towards the front of the cabinet remain close to the ambient and are only minimally affected by the heat dissipated by the power supplies. The total current requirement for this system, including the circulating pump, disk drive, fan and thermoelectric cooler, is approximately 3.75 A at 110 V.

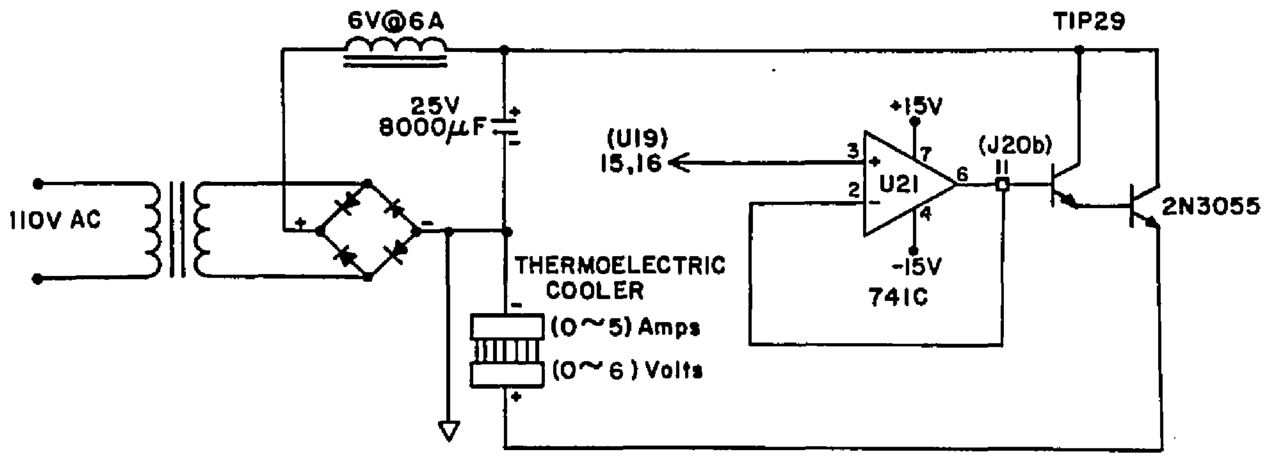

Figure (22). The circuit diagram of the power supply for the thermoelectric cooler.

Table (3). The power supply requirements of the calibration system.

Device	+5	+24	+15	+12 (Volts)	-15	-12	-5
				(Amps)			
AIM-65	2.0	0.5	---	---	---	---	---
Disk Drive	0.8	1.3	---	---	---	.05	---
Disk Controller	0.6	---	---	.13	---	---	---
16-channel Multiplexer	.75	.04	---	---	---	---	---
Data Acquisition and Control Interface	.04	---	0.1	.01	.01	.01	.02
Block heaters	---	.75	---	---	---	---	---
Total Current (Amps)	4.19	2.59	0.1	.14	.01	.06	.02

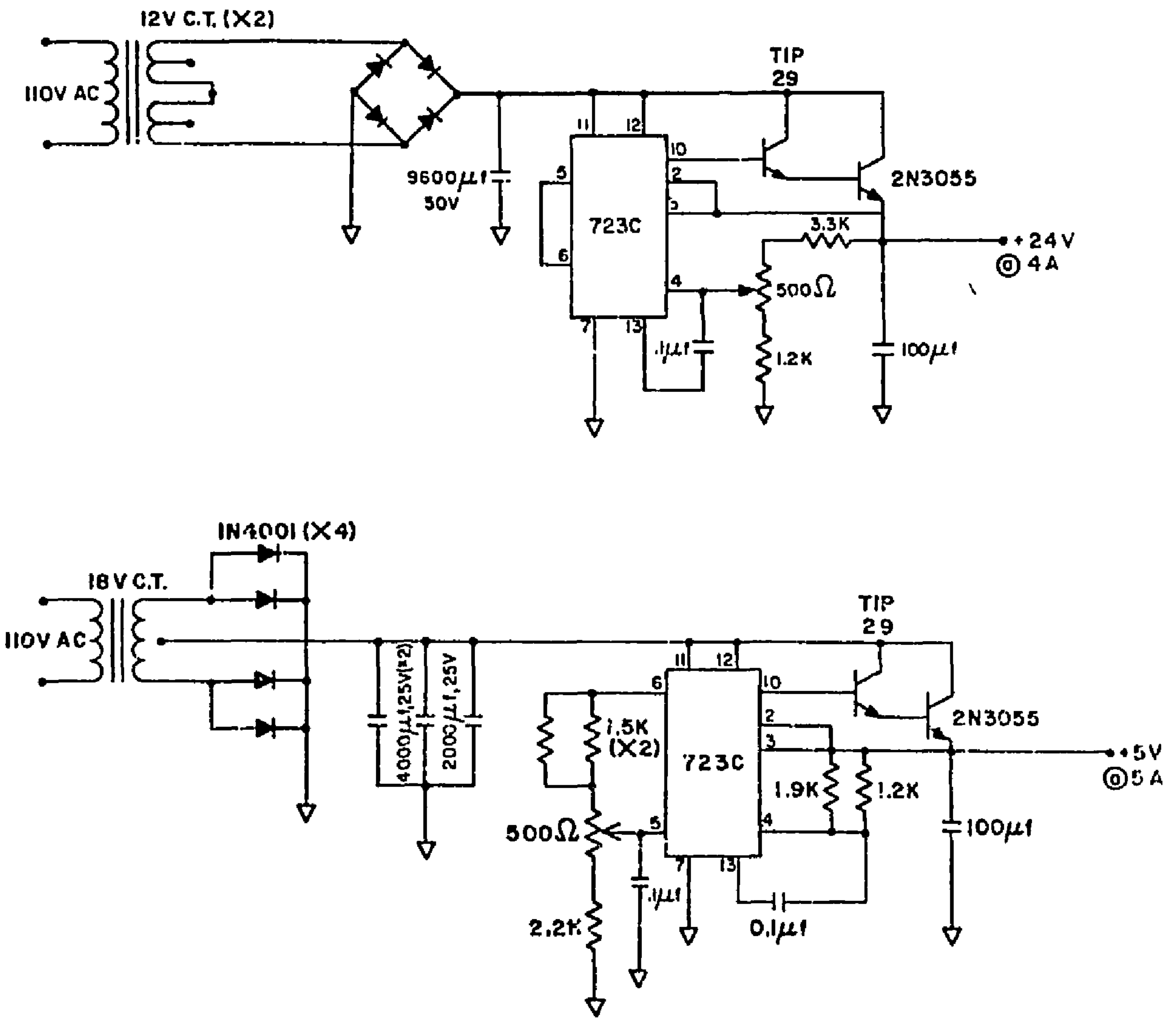

Figure (23). The circuit diagram of the +5V and +24V power supply.

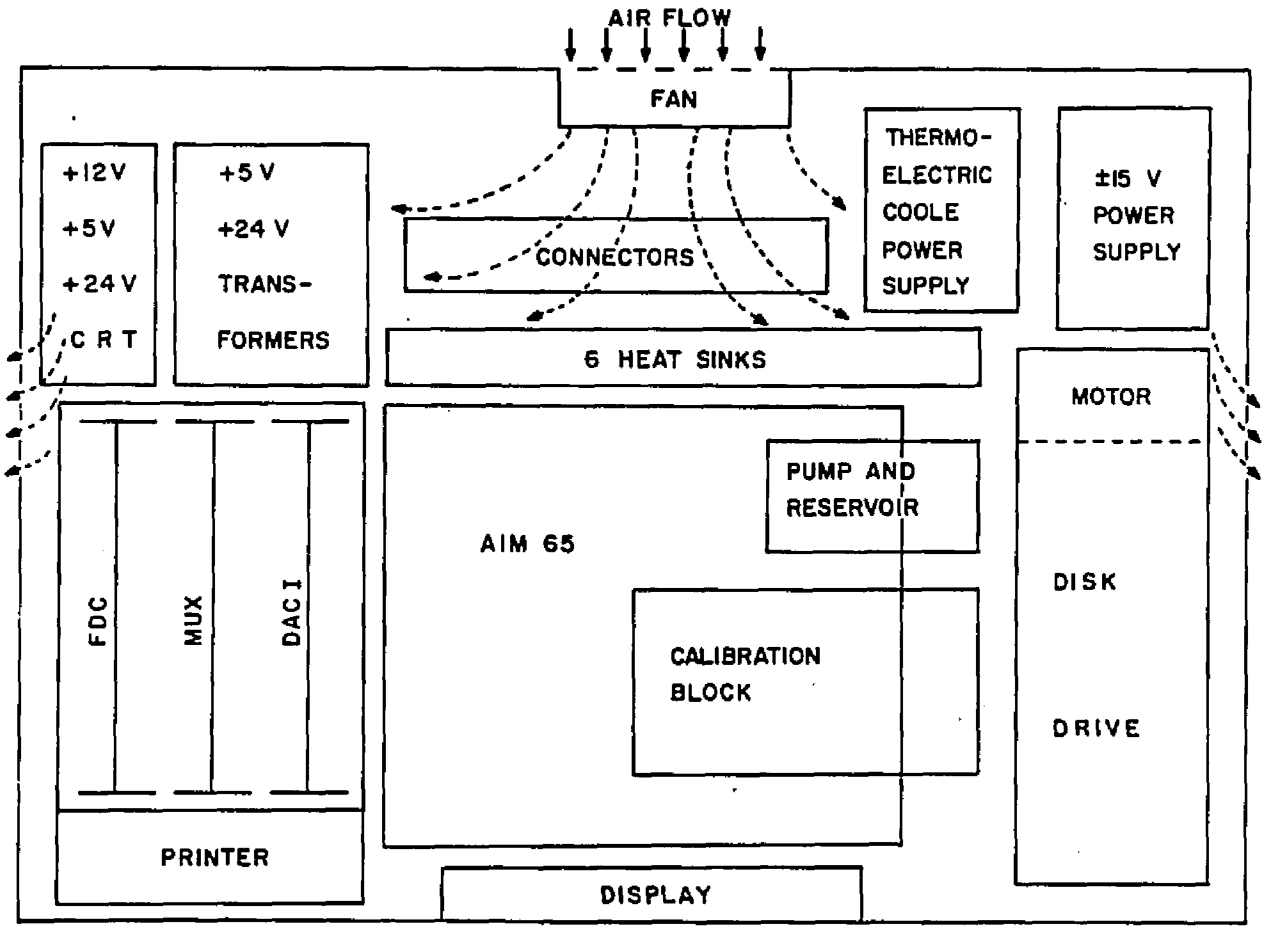

FDC = floppy disk controller
MUX = 16-channel multiplexer
DACI = data acquisition and control interface

Figure (24). The physical layout of this system.

SOFTWARE

The software required by the calibration system can be classified into three main categories, namely, computation, process control and I/O handling. The computation and process control routines are developed specifically for this application whereas the I/O handlers are mostly subroutines available on the AIM-65 monitor. A list of the available system I/O subroutines with their corresponding addresses are shown in Table 7-13 of the AIM-65 User's Guide. A listing of these programs and the AIM-65 monitor is included in the AIM-65 Monitor Program Listing Handbook. A listing of the computation routines and the control routines are contained in a supplement of this thesis : "An Automated Thermistor Calibration System - Program Listings". The computation routine contains approximately 1700 lines of listings and 2.27 K-bytes of assembly code. The control program has about 1600 lines of listings and 2.78 K-bytes of assembly code.

Computation Routines

The 6502 microprocessor itself is very limited in high accuracy computations. It can only add and subtract bytes in binary or BCD format. Therefore programs have to be developed to perform the various calculations required during the calibration process. The basic functions required by the thermistor equation and the control routines include add, multiply, divide and natural logarithm. Since the A/D used has a

BCD output and the 6502 can add and subtract in BCD mode, all calculations are carried out in that format. Thus the difficulties involved in debugging the software during system development, as well as the conversions involved for data display in the conventional decimal format, are both minimized.

As required by the accuracy of the system, most computations are carried to 16 significant digits. Seven digits are sufficient in natural logarithm to maintain accuracy. However, because of the amount of time involved in its implementation, the algorithm used carries less than eight digits of accuracy. As shown in figure (25), the operands involved in these functions each occupy ten bytes: eight bytes for the mantissa and two for the signs and exponent. Due to the many numerical constants involved in the various calculations and the number of temporary results generated by intermediate calculations, fourteen 10-byte working registers are allocated for computational purposes. Table (4) consists of a list of the names and addresses of these registers and their specific functions. The first two registers, ACC and REG1 are mainly used for storing the operands of the functions to be processed and all results are returned to ACC. The X and Y registers in the 6502 are used as pointers for identifying these registers in the various operations. Other routines such as moving operands among registers, normalizing operands or changing signs also must be configured into the software.

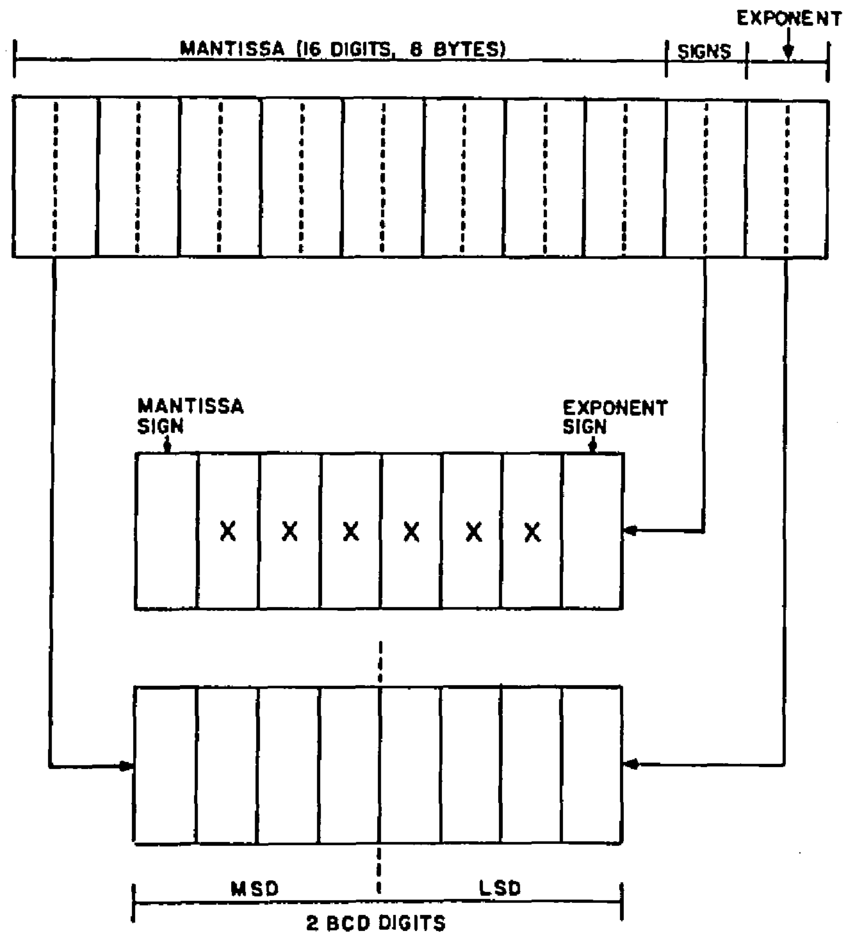

Figure (25). Operand format - the standard form.

Table (4) The addresses of the registers and their specific functions.

Address (hex)	Register	Assigned functions
1Ø	ACC	input:add, divisor, multiply & Ln output:all results
1A	REG1	input:add, divider, multiply
24	A11	A_0 of thermistor equation
2E	A21	A_1 of thermistor equation
38	A31	A_2 of thermistor equation
42	A12	inner block averaged temperature
4C	A22	outer block averaged temperature
56	A32	set temperature
6Ø	A13	current reversal temporary register
6A	A23	current reversal temporary register
74	A33	current reversal temporary register
7E	C1	Ln working register
88	C2	Ln working register
92	C3	constant 1K Ω value
9C	detr	instantaneous temperature of inner or outer block and Ln working register

Any register can be used as input registers for the multiplication routine or as a general purpose working register.

Addition

The first step involved in addition is to check the signs of the exponents of both operands and normalize their mantissas to the same order of magnitude. Then, based on the signs of the mantissas, the normalized numbers are either added or subtracted. After the addition or subtraction, the result is again normalized to the standard form as shown in figure (25) with the signs of the mantissa and exponent adjusted accordingly. Since both positive and negative numbers are allowed in this addition routine, subtraction can be implemented by simply changing the sign of the mantissa in one of the operands.

Multiplication

Multiplication involves the shifting of bits and digits in the operands and the summation of partial products and sums to form the final product. When two 16-digit numbers are multiplied, a 32-digit product is formed. Since only 16 digits of accuracy is required by the system, the computation time can be greatly reduced by eliminating the various steps that have no contribution to the significance of the higher 16 digits. This scheme is shown in figure (26). The first partial product is formed by multiplying the two most significant digits (MSD) of the multiplicand to the least significant digit (LSD) of the multiplier. The next partial product involves the first three MSDs of the multiplicand and the seconcd LSD of the multiplier, and so on until the MSD of the multiplier is encountered. Because of the

```
                                                 A B C D E F G H I J K L M N O P
                                              X  a b c d e f g h i j k l m n o p
       ----------------------------------------------------------------------------
                                            Ap Bp
                                         Ao Bo Co
                                      An Bn Cn Dn
                                   Am Bm Cm Dm Em
                                Al bl Cl Dl El Fl
                             "                Gk
                          "                   Hj
                       "                      Ii
                    "                         Jh
                 "                            Kg   [lower 14 digits ignored]
              "                               Lf
           "                                  Mc
         Ad Bd Cd Dd Ed Fd Gd Hd Id Jd Kd Ld Md Nd
      Ac Bc Cc Dc Ec Fc Gc Hc Ic Jc Kc Lc Mc Nc Oc
   Ab Bb Cb Db Eb Fb Gb Hb Ib Jb Kb Lb Mb Nb Ob Pb
∑  Aa Ba Ca Da Ea Fa Ga Ha Ia Ja Ka La Ma Na Oa Pa
-----------------------------------------------------
C1 C2 D3 D4 D5 D6 D7 D8 " " " " " " " " " D18
```

Figure (26). The formation of product without calculating the lower 14 digits.

initial two-digit offset, all the digits in the multiplicand are involved in the last two partial products.

Before the operation starts, both the multiplier and multiplicand are unpacked into two separate 16-byte registers and a cumulating resigter of 18 bytes long is nulled. Each time a partial product is generated, it is added into this cumulating register to form the final product. The formation of the product is explained in figure (27). It involves the left shifting of bits in the multiplicand digits and the right shifting of bits in the mutiplier digits. As the bits of individual digits in the multiplicand are shifted left, the value of the digit is doubled. Thus if the multiplicand digit = 7 (ØØØØ Ø111) and the multiplier digit = 9 (ØØØØ 1ØØ1), by shifting the bits in the multiplicand digit left, 14 (ØØØØ 111Ø), 28 (ØØØ1 11ØØ) and 56 (ØØ11 1ØØØ) are resulted. As the multiplicand bits are shifted left, the multiplier bits are shifted right. If the least significant bit (LSB) of the right shifted digit is "1" then the left shifted multiplicand digit is added to the cumulating register as a partial-partial product. Thus in this case (7 X 9), there are two partial-partial products, 7 and 56. The partial sum is 7 + 56 = 63. The same process is repeated for all the digits involved in the formation of the partial product. Finally the cumulated partial products are repacked and normalized to the standard form as shown in figure (25).

Division

Division is implemented by repeatedly subtracting the divider

```
If        A B C D                                   3 7 4 2

     X          n                           X           9
__________________________            ___________________________

Then A = ØØØØ ØØ11 = 3
     B = ØØØØ Ø111 = 7
     C = ØØØØ Ø1ØØ = 4                                       18-byte
     D = ØØØØ ØØ1Ø = 2                                     accumulator
                                                       initialized to 0
     n = ØØØØ 1ØØ1 = 9

Procedure:               after some steps                 accum=x
____________________________________________________________________________

1.   (D=2)        ØØØØ ØØ1Ø =2
  a. shift n      ØØØØ Ø1ØØ        1     accum D          x+2

  b. shift D      ØØØØ Ø1ØØ =4
     shift n      ØØØØ ØØ1Ø        0     nop

  c. shift D      ØØØØ 1ØØØ =8
     shift n      ØØØØ ØØØ1        0     nop

  d. shift D      ØØØ1 ØØØØ =16
     shift n      ØØØØ ØØØØ        1     accum D          x+2+16=x+18

2.   (C=4)        ØØØØ Ø1ØØ =4
  a. shift n      ØØØØ Ø1ØØ        1     accum C          x+18+40=x+58

  b. shift C      ØØØØ 1ØØØ = 8
     shift n      ØØØØ ØØ1Ø        0     nop

  c. shift C      ØØØ1 ØØØØ =16
     shift n      ØØØØ ØØØ1        0     nop

  d. shift C      ØØ1Ø ØØØØ =32
     shift n      ØØØØ ØØØØ        1     accum C          x+58+320=x+378

============================================================================

             [similar process continues with A & B]
*nop   = no operation
 accum = accumulate value into cumulating register
```

Figure (27). The formation of partial products by bit shifting.

from the divisor and the left shifting of the divisor until a 16-digit quotion is formed. Each time when the divider is subtracted from the divisor, a counter is incremented. When the difference is negative, the value of the counter is put into the corresponding digits in the quotion. After the quotion is formed, the signs are adjusted and the result is normalized. This process resembles the method of dividing by long hand.

Natural logrithm

Natural logrithm is implemented with a power series expansion, $\log(1+x) = a_1x + a_2x + \ldots + a_7x + a_8x = Ln(1+x)/Ln10$; where

$a_1 = 0.9999964239$	$a_5 = 0.1676540711$
$a_2 = -0.4998741238$	$a_6 = -0.0953293897$
$a_3 = 0.3317990258$	$a_7 = 0.0360884937$
$a_4 = -0.2407338084$	$a_8 = -0.0064535442$

Since this series is only valid for $0 < X < 1$, scaling factors must be used when $X > 1$. For example, $Ln(5432.1) = Ln(1+.358025) + 3Ln(10) + 2Ln(2)$. Thus factors of Ln(10) and Ln(2) are used, when $(1+x) > 2$. With eight terms in the power series, less than eight significant digits are obtained. Since the coefficients $a_1 - a_8$ have 10 significant digits and the A/D has 5-1/2 significant digits, 15-1/2 digits of resolution results in the multiplication of the a_x terms, which has the same width as the designated computation registers. Taking into account the round offs involved, this algorithm provides 7-1/2 digits of accuracy. If higher accuracy is required, more terms would have to be included in the power series. However as the number of terms increases, the computation time increases exponentially.

Process Control

The software involved in controlling the calibration process is divided into four main sections - initialization, interface, control and data acquisition. Appendix B shows a simplified block diagram of the operating procedures for this system. The initialization routine consists of the various messages involved in setting up the system and bringing it through an instrumental calibration. The actual handshake and control of the A/D and D/As are implemented by the interface program. The control routines include the procedures and algorithms involved in temperature control of the block cylinders. When the block cylinders are equilibrated, the temperature of the standard thermometer and the resistances of the various thermistors are sampled and stored by the data acquisition routines.

Current reversal technique is used on all voltage readings. The system first reads the forward and the reverse voltages and then calculates their difference $(IR+V_{emf} - (-IR+V_{emf}))=2IR=2V_{ch}$, see figure (2). In the sampling sequence, the system always starts with channel five which has a constant 999.984 Ω resistor on it. After reading the voltage on this channel, it reads the voltages on the standard thermometer channel, the outer block sensing thermistor channel and the rest of the thermistor channels. Thus the resistance of the various thermistors can be determined by $R_{ch} = [2(V_{ch})/2(V_{1K})](R_{1K})$, where ch=channel. By using this approach, the long term drifts of the op-amp involved in the constant source is eliminated from the measurements ($R_{ch} = V_{ch}/I_{cst}$). Furthermore, by incorporating a linearization algorithm as described in figure (28), the non-linearity errors in most of the electronics can also be minimized.

Initialization

In the initialization program, the system first prompts the operator for the number of thermistors to be calibrated. After that it proceeds through a series of instrumental calibration procedures which nulls the non-linearities and long term drifts of the system. On each thermistor channel are two low temperature coefficient resistors, nominally of 3.5 KΩ and 660 Ω , connected to a selectable toggle switch. These resistances represent the high and low resistance extremes of the thermistors over the range 20°C - 60°C. The system prompts the operator to switch these channel resistance switches at different points in the instrumental calibration process and the voltages of both the high and low resistances are read and stored. The system then calculates the resistance from the stored voltages and linearizes them with respect to their actual resistance as shown in figure (28) so that system drifts and non-linearities can be minimized. After all the linearized resistances are calculated, they are compared to their respective true resistances. If the error involved in any channel is greater than 0.5 Ω , principally due to insufficient warm up, the operator is requested to perform a recalibration. If system drifts

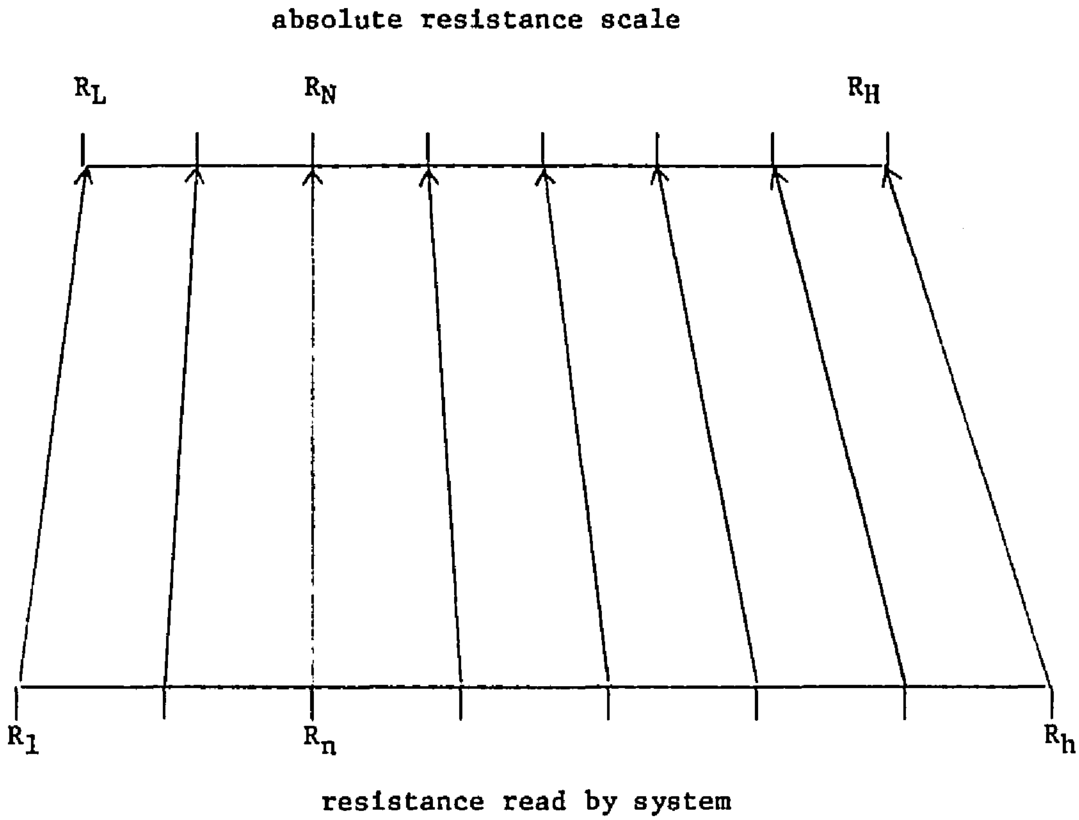

R_L and R_H are known resistances

R_n are measured values

R_1 and R_2 are measured and stored values

R_N are resistances calculated by algorithm

$$\frac{(R_H - R_L)}{(R_h - R_l)} = \frac{(R_N - R_L)}{(R_n - R_l)}$$

$$R_N = \frac{(R_H - R_L)(R_n - Rl)}{(R_h - R_l)} + R_L$$

Figure (28). The linearization algorithm.

and non-linearity errors cannot be reduced to less than 0.5 Ω with this linearization algorithm, a calibration in the hardware is required. When the instrumental calibration is completed, the operator is requested to input the calibration points. The process control routines then take the system through the thermometer calibration independent of any further operator interactions.

Interface

The interface subroutines consist of the timing procedures that control the reading and writing of the A/D and D/A channels. For the thermistor channels, the channel number is loaded into port A and is enabled by raising CB2. Approximately 80 ms are allowed for the mercury-wetted switches to activate. At the end of this delay, CB1 is raised, which produces a leading edge that starts the conversion cycle on the A/D (refer to figure (15) for the timing sequence). The system then returns to the control routine to process the data from previous conversions. When the control process routine is ready to read new data, it will check on SCC of the A/D. SCC is connected to CA1 which is programmed to set its interrupt flag on a leading edge. The completion of a conversion is indicated by this flag on the interrupt flag register(IFR) of the VIA. When the conversion is completed, three DMC pulses are sent by program controlling CB1 in its manual mode through the peripheral control register (PCR). This updates the new data from the internal counters in the A/D into its output latches. When this is done, a trailing edge on $\overline{\mathrm{DAV}}$ will set the CA2 interrupt flag in the IFR. Thus by checking this flag, "datavalid" ($\overline{DAV}$) is confirmed. At this point, the system sends out six DMC pulses on CB1. Each DMC pulse updates a BCD digit from the output latches into the output buffer of the AD7555. Thus the corresponding digit can be loaded into port A and stored. After all digits are read, the routine returns to the control program so that either another conversion can be started or data can be processed. The 6522 VIA and AD7555 data sheets should be consulted for details in the timing and operation of both devices.

The other responsibility of this interface routine is to load the data from port B into the D/As by activating their corresponding channel addresses. When the channel is activated, the data at port B are transparent to the latches in the corresponding D/A. As soon as that channel is deactivated, the data are latched into the D/A. Thus the D/As can be loaded or the data on port B can be changed without affecting any other channel except the activated one.

Control

The control program takes over as soon as the system receives all the calibration points from the operator via the keyboard. This program is divided into four stages namely, initialization, full power, controlled power and constant power.

In the initialization stage, the program samples the initial temperatures of the inner and outer block cylinders and stores them in memory. It also initializes the equilibration counters of both block cylinders, the full power voltages for both heaters and the set temperature of the calibration point into the corresponding registers. After this, it enters the full power stage. Maximum power is applied to heating elements on both blocks. The system samples and displays the temperatures of the block cylinders, on the the AIM-65 digital display. Just before a new temperature is sampled, the present temperature reading is averaged with its previous temperatures. Thus the system only stores and displays the average temperatures even though the instantaneous temperatures are used in calculations. It remains in this mode until the average temperatures of the block cylinders are within 0.6°C of the set temperature (calibration point). The program then switches from full power to controlled power stage.

In the controlled power mode, the system samples the temperature of both block cylinders and adjusts the power to the heating elements continuously until the block cylinders reach equilibrium. The amount of power required is approximated with equations which were determined by a series of experiments that characterize the best heating and control sequences. The power for the inner block is approximated by $\Delta T \times 10$ and the outer block by $(\Delta T \times 20) + (T/1000+0.1)(T-26.85)$,

where ΔT = the difference in temperature between the average and the sampled temperature of the inner or the outer block cylinder.

T = sampled temperature of the outer block cylinder.

The only varying factor involved in the equation for the inner block is ΔT. As the inner block approaches thermal equilibrium, ΔT

gradually decreases. When ΔT gets smaller than the resolution of the D/A, the amount of power applied to the inner block gradually reaches a constant.

The equation which approximates the power to the outer block consists of two terms. The first term is basically the same as that for the inner block except that it has a multiplying factor of 20 due to its weight and size as compared to the inner block. The second term approximates the amount of heat loss through the foam and block assembly. 26.85°C(300 K) is used as the average ambient temperature around the outer container and (T-26.85) represents the temperature difference between the outer block and the ambient (which is the same as the temperature difference between the inside and outside surface of the foam). The thermal conductivity of the foam and block assembly as a function of the temperature of the outer block cylinder is approximated by (T/1000+0.1). Only the thermal conductivity (K) and the temperature difference (ΔT) terms are used in calculating the heat loss ($\dot{Q}$) to the foam. The $A/\partial x$ term (see chapter three), approximately 1.5, is not included in determining the heat loss in the foam. Thus the amount of power determined by this equation is always lagging the actual requirements and overheating of the block cylinders are prevented.

Due to the characteristics of the block, the relationship of the power output of the heaters to the voltage output of the D/A is approximately linear at high powers as shown in figure (29). Thus, simple linear computations only are required for the control algorithm

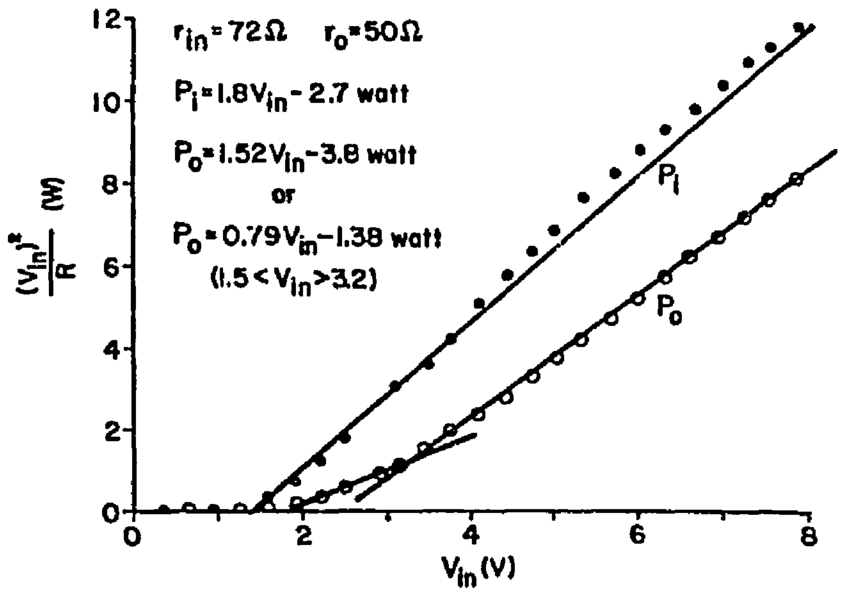

V_{in} = voltages at the output of the D/As

P_i = power applied to the inner block

P_o = power applied to the outer block

r_{in} and r_{out} are the resistances of the inner and outer block heating element.

Figure (29). The voltage and power relationship of the D/As and the heating elements in the inner and outer block cylinders instead of the expected square root function from the V^2 or I^2 terms. Thus both software and computation time are reduced.

During the controlled power stage, the temperature of each block is read and compared with the average of the previous readings. If this difference, ΔT, is less than 0.007°C, the respective equilibration counter for the block cylinders are decremented, otherwise they are incremented. These equilibration counters are initially set to 32 (hex 20). As the control process proceeds, they are adjusted dynamically to compensate for the intrinsic thermal time constants of the block cylinders so that sufficient time is allowed for the block to equilibrate. The process continues until both counters reach zero. The system then switches into a constant power mode which holds the power on both block cylinders at a constant level for approximately two minutes. During this stage no sampling is performed. At the end of the two minutes, the data acquisition cycle is started. In this cycle, the voltages of the 1 K Ω standard resistor, the standard thermistor, the outer block sensing thermistor and the various thermistor channels are read sequentially, each one sampled with the current first forward then reverse. The reading sequence then is reversed and all probes and the standards read again ending with the standard resistor. The average temperatures of the block cylinders and the resistances of the thermistos are calculated and printed on the thermal printer.

The controller then proceeds to the next calibration point, repeating the same process through the last specified calibration point. Finally, the results of the entire calibration are tabulated and the system control is return to the AIM-65 monitor.

RESULTS

This system is designed to calibrate eight thermistors to an accuracy of ± 0.025°C. It is easy to operate and compact in its construction. The testing of this system consisted of three main parts, hardware testing (burned-in) and calibrations, software verification and final testings. They were performed at the various stages during the development of the system.

The operations of the computation and control routines were both verified at the different stages of system development. More than 50 test runs on the calibration process have been performed and different sections of the various programs were checked or verified. In a typical calibration run, approximately 1000 calculations (add, subtract, multiply and divide) are made per minute. No obvious error was detected in neither the computations nor the control process.

The accuracy of the calibrations were tested by two sets of thermistors. The first set consists of eight thermistors with known calibrations and the other consists of 16 new thermistors. The first set was calibrated five times in the automated system over a five day period. The results were compared against the original calibrations in the manual calibration facility and compared against each other for day to day drifts. The second set was calibrated twice. Finally both sets were checked in a gallium melting-point cell (29.771°C) and at 45.3°C against the standard thermometer of the manual calibration apparatus. Table (5), (6) and (7) show the typical results obtained from these series of calibations. The root mean square deviation (RMSD) of these calibrations are also shown in each table. The overall absolute accuracy is ± 0.02°C except in a few cases where the individual channels were not calibrated precisely. These latter show ± 0.03°C or less error. In most cases, when the system is sufficiently warmed up and the channels are precisely calibrated, the accuracy of the calibrations are better than ± 0.015°C throughout the range 25°C - 50 °C.

The amount of time required for a 5°C heat up and equilibration is approximately 20-30 minutes. For a six point calibration run, 2-3 hours is required. A typical equilibration curve of the inner and outer block cylinders is shown in figure (30), they both represent critical damping. The system can be brought to temperature quickly by active control, but equilibration depends on intrinsic time constants. The steady part of the curves are mainly due to the intrinsic thermal time constants of the block and the lag time involved in temperature control. The constant power stage is incorporated mainly to ensure that thermal gradients and pulses induced as a result of the control process are stabilized before the sampling of the calibration results. Finally the current reversal techniques, the integrating A/D, the forward and reverse sampling sequences incorporated in data acquisition average out the various drifts and noise during the control and sampling process.

Table (5). Temperature difference in °C of eight thermistors calibrated on this system compared against the original calibration of each, respectively at 25°C and 50°C.

25°C RMSD = 0.0091°C

Thermistor #	cal 1	cal 2	cal 3	cal4	cal5
6638	-.001	-.012	.001	.005	.012
6598	.002	-.001	-.004	.010	-.008
5966	.012	-.002	.013	.001	.005
6636	.004	-.002	.005	.009	-.005
6600	.005	.009	.002	-.004	.025
6634	.007	.008	.004	.005	.004
6601	-.007	-.003	.015	.006	.003
6635	-.017	-.002	-.001	-.017	-.019

50°C RMSD = 0.0153°C

Thermistor #	cal 1	cal 2	cal 3	cal 4	cal 5
6638	-.003	.006	.023	.025	.011
6598	-.006	.013	.017	.015	.009
5966	.004	.026	.025	.013	.022
6636	.013	.009	.024	.025	-.003
6600	-.002	.011	.002	.003	-.016
6634	-.006	.018	.019	-.019	.010
6601	-.006	$\boxed{-.053}$	.024	$\boxed{.033}$	.021
6635	-.018	-.006	.003	-.001	-.018

$\boxed{}$ loose connector or setup problem, excluded from RMSD calculation.

Table (6). A gallium melting-point check of the thermistors calibrated on this automated calibration system.

Thermistor #	Temperature(°C)	Difference(°C)
6638	29.776	.003
6598	29.780	.007
5966	29.770	-.003
6636	29.768	-.005
6600	29.772	-.001
6634	29.770	-.003
6601	29.768	-.005
6635	29.788	.015
7071	29.766	-.007
7088	29.772	-.001
7090	29.767	-.006
7092	29.765	-.008
7089	29.760	-.013
6326	29.782	.009
6325	29.767	-.006
6623	29.767	-.006
6322	29.774	.001
6324	29.769	-.004
3793	29.772	-.001
6633	29.774	.001
6645	29.778	.005
6641	29.768	-.005
6643	29.790	.017
6644	29.764	-.009

RMSD = 0.0073°C

Difference = thermistor temperature - gallium cell temperature
gallium cell temperature = 29.773 ± .002°C

Table (7). A comparison of the thermistors calibrated on the automated system against the standard thermometer in the manual system.

Thermistor #	Thermistor temperature (°C)	Standard thermometer temperature (°C)	Temperature Difference (°C)
6638	45.305	45.299	.006
6598	45.318	45.301	.017
5966	45.297	45.301	-.004
6636	45.274	45.301	-.027
6600	45.309	45.310	.008
6634	45.315	45.310	.005
6601	45.305	45.301	.004
6635	45.321	45.300	.021
7091	45.279	45.301	-.004
7088	45.280	45.302	-.022
7090	45.295	45.301	-.006
7092	45.295	45.302	-.007
7089	45.285	45.302	-.017
6326	45.331	45.329	.002
6325	45.309	45.329	-.020
6623	45.320	45.329	-.009
6622	45.321	45.339	-.018
6324	45.325	45.329	-.004
3793	45.243	45.241	.002
6633	45.291	45.285	.006
6645	45.287	45.285	.002
6641	45.301	45.301	.000
6643	45.308	45.287	.021
6644	45.290	45.301	-.011

RMSD = 0.0128°C

* Temperature difference = thermistor - standard thermometer

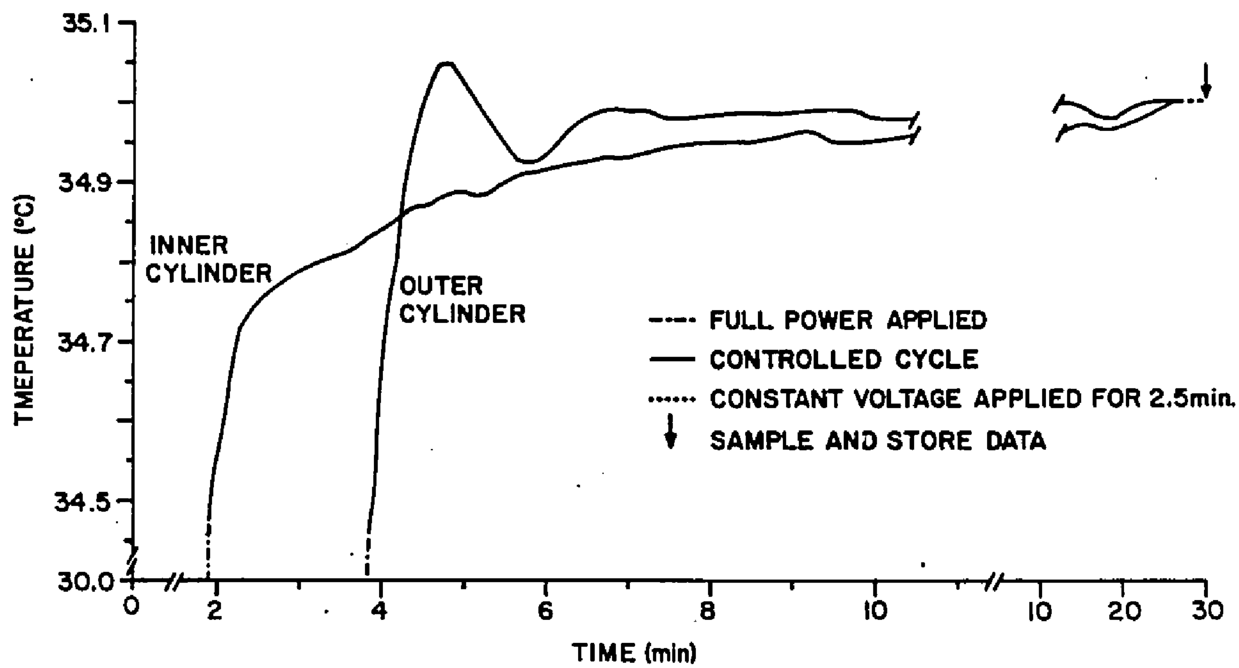

Figure (30). A typical equilibration curve of the block cylinders.

DISCUSSION

The primary goal of this project was to design and construct an automated thermistor calibration system for the applications involved in hyperthemia. However, there are a few minor improvements which can be incorporated into this calibration unit that would certainly upgrade this system into a better version.

Initially the space between the inner and outer block was just an air gap, which had a rather long equilibration time constant (more than an hour). Crushed aluminum foil was inserted into this gap to increase thermal conduction between the two block cylinders and the equilibration time was reduced to approximately 20 - 30 minutes. If another calibration block is to be designed in the future, it would be better to seal the bottom of the outer block cylinder and fill the gap between the two block cylinders with fluid such as mineral oil. This would reduce the effort involved in cooling the block to below ambient temperatures by incorporating a cooling coilng in the fluid and run ice-cooled water through this coil.

The drivers for the heating elements and the D/As that control the heaters can be incorporated as part of the calibration block. The required power supply voltage inputs and interfacing signals can be brought to the 25 pin connector presently mounted on the side of the block. This would make the calibration block a completely stand alone unit which could be interfaced to other types of microprocessor or digitally controlled systems.

The thermoelectric cooling unit is very inefficient in cooling the calibration block to temperatures lower than 25°C. Some redesign is required to improve the efficiency of the present method of heat extraction from the block cylinders. When the thermoelectric cooler is operating, the temperature inside the cabinet is raised by 3 - 5°C. This creates minor drifts in some of the sensitive electronic components. Thus the thermoelectric cooler should be eliminated in the future. After a few experiments, air or tap water cooling was found to be more efficient than thermoelectric cooling. Chilled air cooling, tap water or ice water cooling as described earlier might be a better choice.

Presently, all the curve fittings are done on a PDP-8 system which contains most of the required programs for the manual calibration system. In order to make this calibration system a more complete unit, the same algorithm can be implemented on the AIM-65. However, it will take much longer to do it in the 6502 machine language code as compared to the 32-bit floating hardware that is available on the PDP system.

If a higher quality A/D with less non-linearity and drift errors are used, accuracies better than 0.01°C could be achieved. However this might increase the interface difficulties if more data and control lines are required than in the present system. Furthermore, more stable and higher resolution A/D's can cost as much as $600 - $800 as compared to monolithic ones which are less than $100. Nevertheless, software compensation is usually not required in better quality A/D's to achieve high precision measurements.

Many electronic thermometers such as thermocouple readers or digital thermistors have either analog or digital ouputs. Thus with some software modification, a selectable switch to disconnect the constant current that flows through the channels, and a scaling of the analog voltages if necessary, these devices could be calibrated readily on any of the eight channels. Digital inputs can be interfaced easily through the parallel I/O port on the VIA.

A good book keeping system that could record the results of every calibration and store them on the disk in a systematic way would eliminate many unnecessary problems. System drifts, thermometer reliabilities or the stability of the standard thermometer could be detected by analyzing the records. If the system could take care of some of these by itself, better reliability and less error would result.

Diagnostic routines which check the various parts of the system are necessary, especially if the system is to be used by persons inexperienced in thermometry or electronic measurements. Thus it would be convenient to have built-in routines that can verify the various operations of the system as a regular maintaince check.

Under certain circumstances, faster calibrations might be more important than higher accuracy. In these cases, a convenient algorithm could be set up to calibrate thermometers with less time and accuracy. For example a calibration of thermocouple systems or optical thermometers would require an accuracy of only 0.1°C. If the calibration could be performed within 30 minutes, then it would be practical to check clinical probes each time before use. Thus quick checks would be possible without going through a precise calibration that takes three hours.

Most of the above mentioned options and improvements are under development now and require only minor changes to the existing system. Finally this system can be made smaller if the various sub-modules can be consolidated. For example, the system power supplies could be orgainzed onto a single printed circuit and a multi-voltage output transformer could be used. The multiplexer and DACI circuitries can be put on a printed circuit board to improve system performance. PROMs (programmable read only memory) could be used to store the calibration routines rather than using a floppy disk, if the results of each calibration were not to be stored. Thus this automatic thermistor calibration unit could be reproduced in a smaller and more compact form. Table (8) consists of a brief cost analysis of the various sub-modules and an estimate of the amount of time spent in developing this system. A duplicate system would have nearly the same component cost, but a much lower labor cost although some development time would be required to complete the above modifications. Subsequent units could then be constructed perhaps in 6 to 10 weeks.

Table (8). A cost analysis of the system.

Device or component		approximate cost
AIM-65		$550
disk drive		$500
disk controller		$650
multiplexer		$150
DACI		$250
thermoelectric cooling unit		$170
cabinet etc.		$300
cables & connectors		$250
power supplies		$200
miscellaneous		$200
Total cost		$3520
system design & experiments	200 hrs	5wks
hardware	600 hrs	15wks
software	800 hrs	20 wks
testing & miscellaneous	400 hrs	10wks
Total hours	2000 hrs	50wks

APPENDIX A

A listing of the results of a calibration after a least squares fit.

This thermistor is designated 6600

BKPGE	SQ	PROBE RESISTANCE	MEASURED TEMPERATURE	CALCULATED TEMPERATURE	TEMPERATURE DIFFERENCE
7	1	2333.620	25.865	25.86568	-0.00068
7	2	2076.810	29.385	29.38452	0.00048
7	3	1759.320	34.523	34.52208	0.00092
7	4	1489.450	39.839	39.83921	-0.00021
7	5	1257.330	45.421	45.42209	-0.00109
7	6	1017.970	52.640	52.63948	0.00052

A_1 = 8.9164280891 E -04

A_2 = 3.0737316608 E -04

A_3 = 1.4778721332 E -07

The RMSD = 0.0007129

(Temperature in °C and resistance in Ω)

APPENDIX B

A simplified block diagram of the calibration procedures involved in this automated thermistor calibration system.

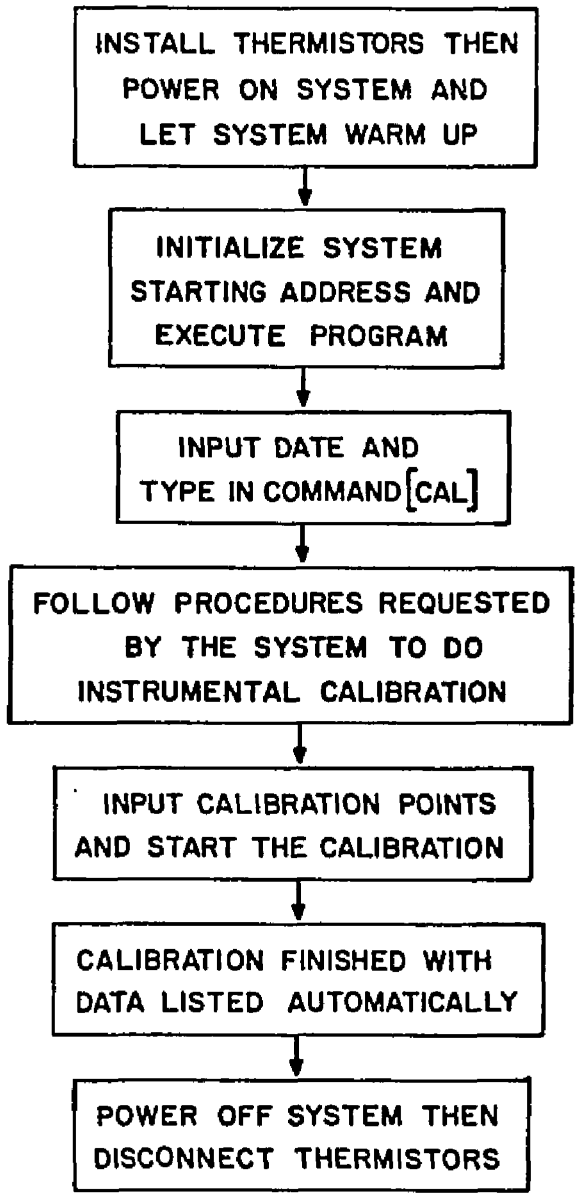

LIST OF REFERENCES

Analog Devices, Inc., Data Acquisition Components and Subsystms, pp. 1-17, 1-25, 1-65, 9-13, 10-57, 1980.

Burr-Brown Research Corporation, General Catalog, pp. 2-22, 1979.

Cetas, T. C. and Connor, W. G., "Thermometry Considerations in Localized Hyperthemia", Medical Physics, vol. 5, pp.79, 1978.

Cetas, T. C., "Thermometry", Therapeutic Heat and Cold, 3rd edition, in press.

Chapman, A. J., Heat Transfer, McMillan, 1960.

Graeme, G., Designing with Operational Amplifier, McGraw Hill, 1978.

Holman, J. P., Heat Transfer, McGraw Hill, 1963.

Huson, R. P., "Measurement of Temperature", Reviews of Scientific Instruments, vol. 51, pp. 871, 1980.

Kimball, C. D. and Harruff, R. W., "Thermistor Thermometry Design for Biological Systems", Yellow Springs Instruments Co. Inc., 1971.

Magnecraft Electronic Co., Designers' Handbook and Catalog of Reed and Mercury Wetted Contact Relays, 1972.

Mangum, B. W. and Thornton, D. D., "Determination of the Tripple-Point Temperature of Gallium", Metrologia, vol 15, 1979

MELCOR (Material Electronic Products Corporation), Solid State Cooling with Thermoelectrics, Catalog - Series FC, 1980.

Micro Technology Unlimited, A Channel Oriented Operating System (CODOS), version 1.2, 1981.

Micro Technology Unlimited, Double Density Disk Controller for KIM/MTU Bus System, Rev. A, May, 1980.

Middleton, W. E. K., A History of the Thermometers, Johns Hopkins Press, Baltimore, 1966.

Motorola Semiconductor Products Inc., Low Power Schottky TTL, Series B, 1977.

National Semiconductor Corporation, Voltage Regulator Handbook, pp. 10-89, pp. 10-119, 1978.

Preston-Thomas, H., "Amended Edition of 1975" ("International Practical Temperature Scale of 1968"), Metrologia, vol. 12, pp. 7, 1969.

Quinn, T. J. and Comptom, J. P., "The Foundations of Thermometry", Reports on Progress in Physics, vol. 38, pp. 15, 1975.

Rockwell International Corporation, AIM 65 User's Guide, 1979.

Rockwell International Corporation, AIM 65 Microcmputer Monitor Program Listing, 1979.

Rockwell International Corporation, R6500 Microcomputer System Hardware Manual, 1978.

Rockwell International Corporation, R6500 Microcomputer Programming Manual, 1979.

Shugart Associates, SA800/SA801 Diskette Storage Drive, OEM Manual, 1977.

Sostman, H. E., "Melting Point of Gallium as a Temperature Calibration Standard", Reviews Scientific Instruments, vol. 48, No. 2, 1977.

Steinhart, J. S. and Hart, S. R., "Calibration Curves for Thermistors", Deep Sea Research, vol. 15, pp. 497, 1968.

Synertek Corporation, MOS Data Catalog, pp. 3-47, pp. 5-3 thru 5-42, 1978.

Texas Instruments Incorporated, The TTL Data Book, 2nd edition, 1976.

Thermometrics, Inc., Thermistors, Catalog No. 181, pp. C7 - C8, 1980.

Trolander, H. W., "The Current State of Electrical Thermometry for Biological Applications", Yellow Springs Instruments Co. Inc., 1971.

Trolander, H. W., et al., "Reproducibility, Stability and linearization of thermistor resistance thermometers", Yellow Springs Instruments Co. Inc., Temperature, vol. 4, No. 95, pp. 997, 1972.

Wood, S. D., Mangum, B. W., Filliken, J. J. and Tillett, S. B., "An Investigation of the Stability of Thermistors", Journal of Research of NBS, vol. 83, No. 3, 1978.